Cell Reports

Article

Transgenerational Sterility of Piwi Mutants Represents a Dynamic Form of Adult Reproductive Diapause

Graphical Abstract

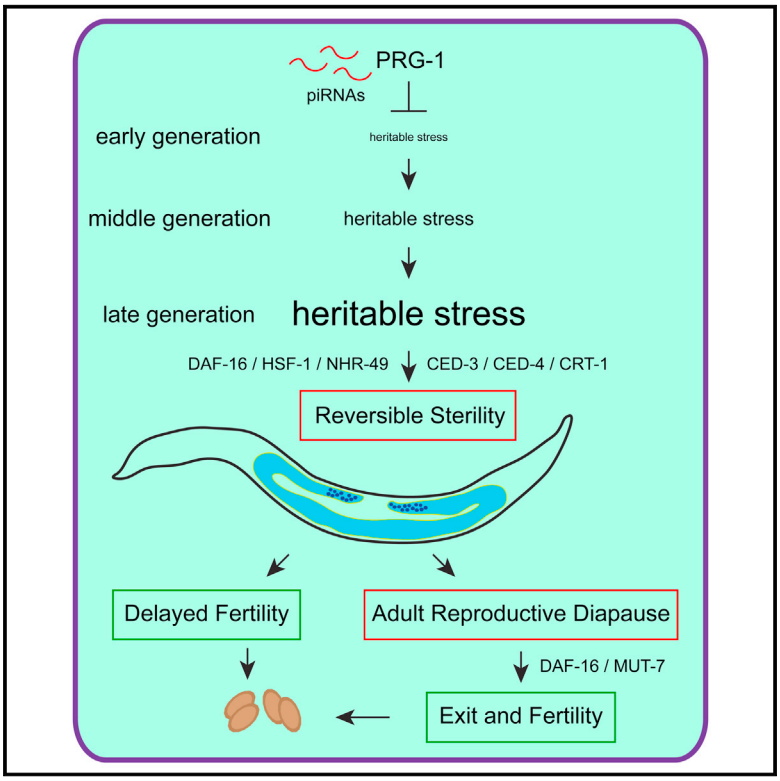

Highlights

- Sterile *prg-1*/*Piwi* mutants display germ cell atrophy in adult germlines
- Indefinitely sterile *prg-1* mutants become fertile when fed alternate food source
- Sterility of *prg-1* mutants is a form of adult reproductive diapause
- *prg-1* mutant sterility may therefore be the consequence of "heritable stress"

Authors

Bree Heestand, Matt Simon, Stephen Frenk, Denis Titov, Shawn Ahmed

Correspondence

shawn@med.unc.edu

In Brief

Heestand et al. examine a form of diapause that occurs in late-generation *C. elegans Piwi/prg-1* mutants. They argue that the sterility of late-generation *prg-1* mutants may be a consequence of "heritable stress." Thus, an endogenous form of stress may be transmitted by germ cells to modulate heredity and fertility.

Heestand et al., 2018, Cell Reports *23*, 156–171
April 3, 2018
https://doi.org/10.1016/j.celrep.2018.03.015

CellPress

OPEN ACCESS
CellPress

Cell Reports
Article

Transgenerational Sterility of Piwi Mutants Represents a Dynamic Form of Adult Reproductive Diapause

Bree Heestand,[1,2,3] Matt Simon,[1,2,4,5] Stephen Frenk,[1,2] Denis Titov,[1,2,4] and Shawn Ahmed[1,2,3,4,6,*]
[1]Department of Genetics, University of North Carolina, Chapel Hill, NC 27599, USA
[2]Department of Biology, University of North Carolina, Chapel Hill, NC 27599, USA
[3]Lineberger Comprehensive Cancer Center, University of North Carolina, Chapel Hill, NC 27599, USA
[4]Curriculum in Genetics and Molecular Biology, University of North Carolina, Chapel Hill, NC 27599, USA
[5]Present address: Department of Biology, University of Rochester, Rochester, NY, USA
[6]Lead Contact
*Correspondence: shawn@med.unc.edu
https://doi.org/10.1016/j.celrep.2018.03.015

SUMMARY

Environmental stress can induce adult reproductive diapause, a state of developmental arrest that temporarily suspends reproduction. Deficiency for *C. elegans* Piwi protein PRG-1 results in strains that reproduce for many generations but then become sterile. We found that sterile-generation *prg-1/Piwi* mutants typically displayed pronounced germ cell atrophy as L4 larvae matured into 1-day-old adults. Atrophied germlines spontaneously reproliferated across the first days of adulthood, and this was accompanied by fertility for day 2–4 adults. Sterile day 5 *prg-1* mutant adults remained sterile indefinitely, but providing an alternative food source could restore their fertility. Our data imply that late-generation *prg-1* mutants experience a dynamic form of adult reproductive diapause, promoted by stress response, cell death, and RNAi pathways, where delayed fertility and reproductive quiescence represent parallel adaptive developmental outcomes. This may occur in response to a form of "heritable stress" that is transmitted by gametes and epigenetic in nature.

INTRODUCTION

Diapause is a state of developmental arrest that promotes survival and delays fertility in response to harsh environmental conditions such as seasonal change or limited nutrient availability (Nystul et al., 2003; Padilla and Ladage, 2012; Schiesari and O'Connor, 2013; Tatar and Yin, 2001). For example, many mammals exhibit some form of in utero embryonic arrest in response to exogenous stress until favorable environmental conditions are encountered, thereby increasing the chance of survival for their offspring. Adult reproductive diapause (ARD) occurs when adults temporarily suspend reproduction in response to environmental stress and has been documented for a variety of invertebrates (Nystul et al., 2003; Padilla and Ladage, 2012; Schiesari and O'Connor, 2013; Tatar and Yin, 2001). *C. elegans* that experience starvation during the final larval stage (L4) can mature into long-lived sterile adults that are in ARD, also termed reproductive quiescence, where germ cell numbers are reduced and reproduction is suspended until food is encountered (Angelo and Van Gilst, 2009). Entry and exit for starvation-induced ARD is influenced by a second environmental stress, population density, which also promotes larval arrest during development (Golden and Riddle, 1982, 1984). Vertebrates, possibly including humans, can also enter a state of suspended animation in response to anoxia (Blackstone et al., 2005), which is plausibly reminiscent of hypoxia-induced embryonic diapause in *C. elegans* (Miller and Roth, 2009). While environmental cues can suspend reproduction in adulthood by activating ARD, it is unclear whether this developmental program can occur in response to an endogenous form of stress.

Germ cells possess the ability to remain eternally youthful as they are transmitted from one generation to the next. Studies of germ cell immortality in *C. elegans* have focused on *mortal germline* mutants that initially display normal levels of fertility, but growth for additional generations results in drops in fertility and eventually in complete sterility (Smelick and Ahmed, 2005). Conceptually, *mortal germline* mutants may transmit a form of transgenerational stress that accumulates over the generations prior to triggering sterility. *C. elegans* telomerase mutants are deficient for *de novo* telomere repeat addition at chromosome ends, and these *mortal germline* mutants transmit telomeres that shorten progressively and ultimately elicit chromosome fusion and genome catastrophe (Meier et al., 2006). Consistently, deficiency for telomerase in mice and humans results in phenotypes that display genetic anticipation and are exacerbated in successive generations (Armanios and Blackburn, 2012). Moreover, telomerase is deficient in somatic cells of normal humans and this triggers senescence after growth for a number of cell divisions, which represents one mechanism to suppress tumor formation (Sharpless and DePinho, 2007). Senescence can also be activated by transcriptional induction of p16/Ink4a, which is a major tumor suppressor protein that responds to many forms of stress and whose expression increases by several orders of magnitude in human and mouse tissues with age, even though inbred mouse tissues have long telomeres and their somatic cells are positive for telomerase. Thus,

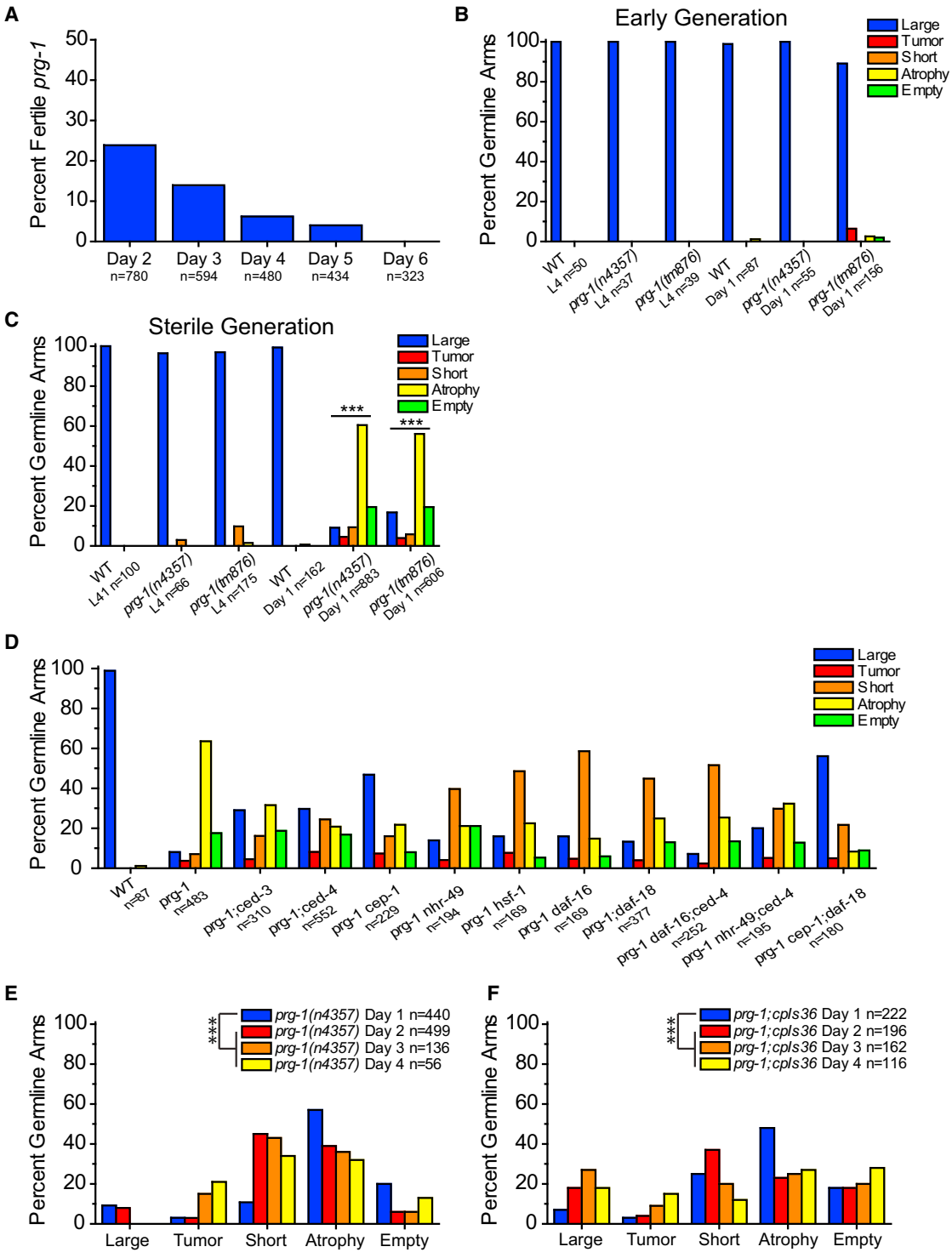

Figure 1. Sterile *prg-1* Animals Exhibit Germline Remodeling

(A) Sterile day 1 *prg-1(n4357)* animals were scored daily for continued sterility from days 2 through 6. Percent fertile are the amount that reversed sterility on each day. n represents total worms scored.

(B) Germline phenotypes of fertile, early-generation (F4) germlines in L4 larva and young adults. n represents total germline arms scored (B–F). Germline categories are defined in Experimental Procedures.

(legend continued on next page)

non-telomeric forms of endogenous stress are relevant to aging (He and Sharpless, 2017; Sharpless and DePinho, 2007), and it is possible that analysis of germ cell immortality pathways could reveal novel forms of stress that are relevant to aging of human somatic cells.

C. elegans PRG-1/Piwi interacts with Piwi-interacting RNAs (piRNAs) in germ cells to promote transgenerational genomic silencing and germ cell immortality (Bagijn et al., 2012; Batista et al., 2008; Das et al., 2008; Simon et al., 2014). However, *C. elegans prg-1* mutants are unlikely to become sterile as a consequence of telomere erosion, as they fail to display telomere fusions near sterility (Simon et al., 2014). This implies that deficiency for PRG-1/Piwi results in accumulation of a distinct form of transgenerational damage.

We previously showed that the transgenerational fertility defect of *prg-1/Piwi* mutants could be suppressed by intermittent or constitutive reduction of the insulin/IGF1 stress response pathway (Kenyon, 2010; Simon et al., 2014). This discovery created a tacit link between an intervention that represses somatic aging and promotes stress resistance in diverse organisms with the transgenerational fertility defect caused by piRNA deficiency (Kenyon, 2010; Simon et al., 2014). Both small RNAs and histone H3K4 demethylases were required for reduced insulin signaling to promote fertility of *prg-1/Piwi* mutants, implying that an epigenomic silencing process can alleviate the piRNA-mediated genome silencing defect of *Piwi* mutants (Simon et al., 2014). How the transgenerational epigenetic defect of *prg-1* mutants elicits sterility, and whether the sterility phenotype might be relevant to stress or aging (Smelick and Ahmed, 2005), remains unclear. Here, we report that *prg-1/Piwi* mutants become sterile via a mechanism that resembles starvation-induced ARD, implying that they succumb to a form of heritable stress, and we provide evidence suggesting that this sterility can be reversed via a small RNA pathway that is promoted by DAF-16/Foxo.

RESULTS

Sterile-Generation *prg-1* Mutants Display Delayed Fertility and Germ Cell Atrophy

The brood size of late-generation *prg-1* mutants becomes small prior to sterility and is accompanied by a high frequency of males that are incapable of mating (0/25 crosses of single *prg-1* mutant males with *unc-13* hermaphrodites were successful, whereas 25/25 analogous crosses with N2 wild-type males were successful). Individual sterile *prg-1* adults were isolated from late-generation populations of animals that had grown for 20–50 generations. When randomly singled, late-generation mothers gave rise to very few progeny; these progeny were often sterile on day 1 of adulthood. In contrast, wild-type controls or early generation *prg-1* mutants (F4) always laid embryos on day 1 (Figure S1B). Interestingly, some late-generation *prg-1* mutant animals that failed to lay embryos on day 1 of adulthood became fertile on day 2 (24%). Of those animals that remained sterile on day 2, 14% became fertile on day 3, 6% of sterile day 3 adults become fertile on day 4, and 4% of sterile day 4 adults became fertile on day 5. When sterile *prg-1* mutant animals became fertile on days 2–5, they each laid only a few eggs, similar to their late-generation siblings that were fertile on day 1. However, after day 5 of adulthood, all sterile animals remained sterile (Figure 1A). We created a *prg-1* mutant strain with a Neon Green transgene, *cpIs36*, which allows the germline to be visualized, and found that similar fractions of late-generation animals that were sterile on day 1 of adulthood became fertile on days 2, 3, 4, and 5, with all day 5 sterile animals remaining sterile (Figure S1A). These data indicate that late-generation *prg-1* mutants consist of two populations of adults that fail to lay embryos on day 1 of adulthood: one in which reproduction eventually occurs during days 2–5 of adulthood and a second that remains completely sterile after day 5 of adulthood.

To study the germlines of sterile-generation *prg-1* mutants, we identified late-generation *prg-1* mutant populations laying very few progeny, and individually isolated hundreds of candidate animals. From the progeny of some of these animals, we could identify sterile day 1 adults along with younger sibling animals likely to become sterile that were available for L4 larval-stage analysis. In both early-generation (F4) and sterile-generation *prg-1* mutant animals, we found that the early L4 larval stage, which immediately precedes adulthood, possessed germlines whose size and developmental stage were generally comparable to those of control wild-type L4 larvae (Figures 1B, 1C, 2A, 2B, and S2A). The germlines of both fertile and sterile late-generation *prg-1* mutant adults were smaller in total length in comparison to wild-type or for early-generation *prg-1* mutants, such that their distal tip cells rarely crossed and their germline bends were premature, which may be consistent with the small brood sizes of fertile late-generation *prg-1* mutant strains (Figures 2, 6A, S2H, and S2I). Some sterile day 1 *prg-1* mutant adults contained large germline arms whose sizes were comparable to those of fertile late-generation siblings and whose developmental transitions were comparable to wild-type (Figure S2F). However, there was a significant change in germline profiles of sterile *prg-1* mutants compared to wild-type (Figure 1C), with most sterile 1-day-old *prg-1* mutant adults displaying a germ cell atrophy phenotype and possessing only a small population of mitotic germ cells near the distal tip cell (Figures 1E, 1F, 2G, 2H, and 2L). Notably, animals that displayed germ cell atrophy were devoid of germ cells at various stages of meiosis (Dernburg et al., 1998), which

(C) Germline phenotypes of sterile L4 larva and young adults. Sterile day 1 adult *prg-1* germline profiles were significantly different than wild-type controls. ***$p < 0.0001$, chi-square test with Bonferroni correction.

(D) Effects of starvation-induced ARD genes and stress response transcription factors on sterile germline phenotypes of *prg-1*. p values determined using pairwise chi-square tests with Bonferroni correction (all comparisons in Table S1).

(E) Germline phenotypes of sterile *prg-1* mutants at day 1, day 2, day 3, and day 4. Scored using fixed DAPI stain. ***$p < 0.0001$, chi-square test with Bonferroni correction between day 1 and all other day germline profiles.

(F) Live score of germline phenotypes of sterile *prg-1* in day 1, day 2, day 3, and day 4 *prg-1:cpIs36* mutants. ***$p < 0.0001$, chi-square test with Bonferroni correction between day 1 and all other day germline profiles. For all panels, data were combined from a minimum of three experiments.

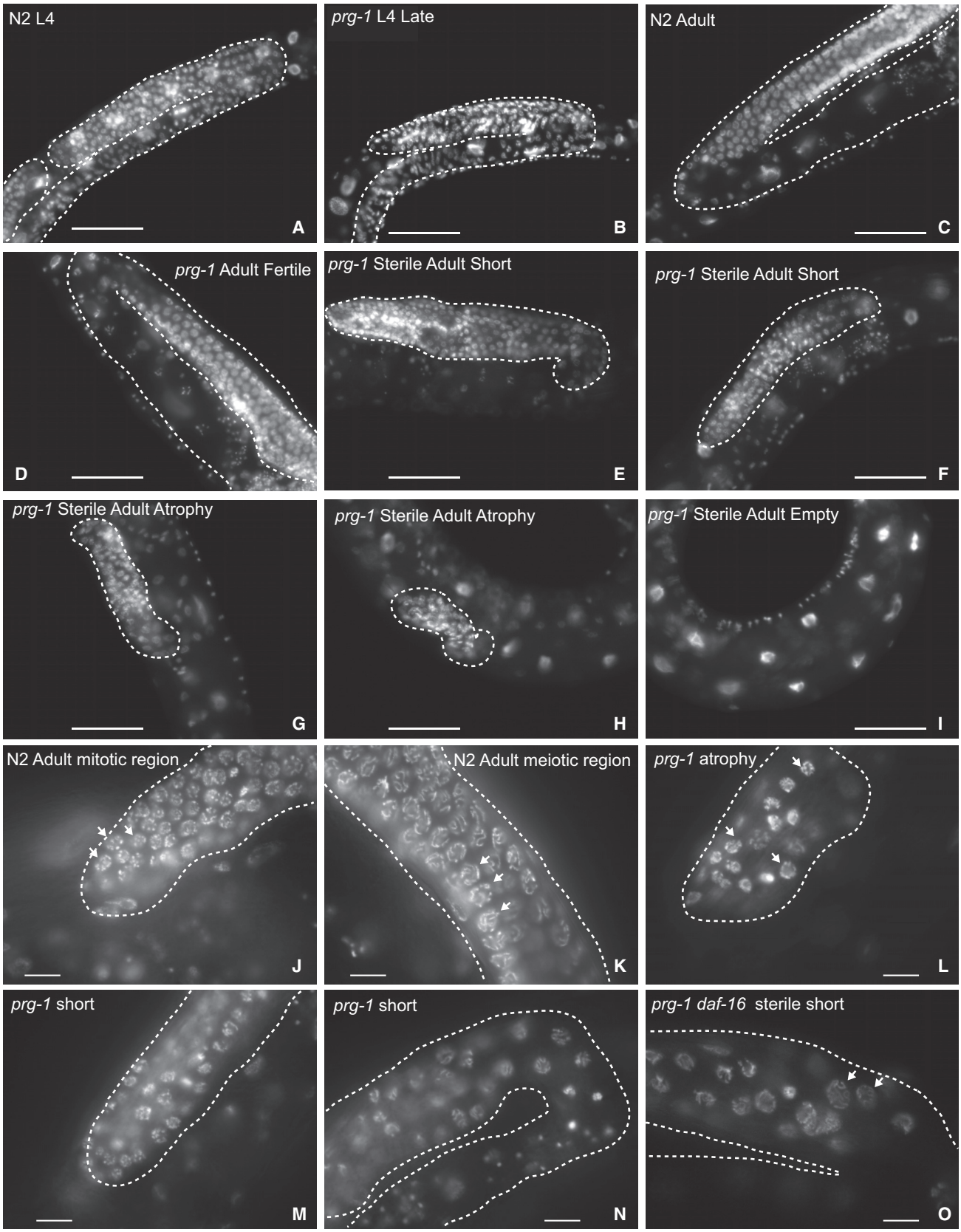

(legend on next page)

were abundant in sterile-generation *prg-1* mutant L4 larvae. Two additional minor fractions of sterile *prg-1* mutant adults either lacked germ cells altogether (empty) or had short germlines with both mitotic and meiotic germ cells (Figures 1C, 1E, 1F, 2E, 2F, 2I, 2M, and 2N). These results imply that a dramatic germ cell atrophy phenotype typically occurs during the L4-to-adult transition for most sterile *prg-1* mutant 1-day-old adults.

We next studied the structure of the germlines of sterile *prg-1* mutants using the transgene *cpIs36*, which expresses *Pmex-5*::*mNeonGreen* brightly throughout the germline. We found that we could enrich for late-generation *prg-1; cpIs36* mutants that give rise to sterile progeny by isolating late-generation parents with small germlines. Sterile day 1 *prg-1; cpIs36* mutant animals were singled and blindly scored for fertility daily and for anterior and posterior germline arm size based on fluorescence detected on agar plates using a stereomicroscope until sterility was reversed or remained completely sterile for 5 days. As a control, we mounted a number of sterile day 1 adults on slides and observed them using a 40× objective. We found that a fraction of germline arms were entirely devoid of germ cells and another fraction contained only a few germ cells, which would be difficult to see at low resolution on the stereomicroscope. Most germline arms that were scored as empty on day 1 remained empty, although some reproliferated and these presumably correspond to sterile day 1 *prg-1* mutant germline arms that were not entirely devoid of germ cells. Most day 1 animals that had atrophied germlines displayed reproliferation of the germline arm. Of those animals in which both germline arms were either atrophied or empty on day 1 of adulthood, 16% became fertile on days 2–5 of adulthood, indicating that germ cell atrophy represents a state of transient sterility. Additionally, the germline arms of all 35 animals that became fertile displayed germ cell proliferation such that none possessed atrophied germlines in both anterior and posterior germline arms on day 2 of adulthood (Figure 3). Moreover, of 35 worms that became fertile, only 4 arms out of 70 scored were in atrophy on day 2, indicating that germ cell proliferation on day 2 was an excellent predictor of reversibility of sterility. Regrowth did not guarantee reversal of sterility since we found numerous examples of worms that regrew their germlines yet remained sterile. Furthermore, while empty germlines generally remained empty, germlines that were either atrophied or short on day 1 of adulthood were dynamic and regrew across the first 5 days of adulthood. When scored either by staining with DAPI or by observing a Neon Green germline reporter, germline arms of sterile day 2, day 3, and day 4 *prg-1* mutant adults displayed a significant change in germline size when compared to sterile day 1 adults, with an increased frequency of short germlines that contained cells in various stages of meiosis in comparison to the number of day 1 atrophied germline arms that were devoid of meiotic germ cells (Figures 1E and 1F). Thus, the germline arms of most sterile-generation *prg-1* mutant adults shrink to a state of atrophy as L4 larvae mature to day 1 adults but then reproliferate. These observations are consistent with the activation of a mechanism to delay the onset of fertility in late-generation *prg-1* mutants.

Apoptosis and Necrosis Promote Germ Cell Atrophy in Sterile *prg-1* Mutants

A pattern of germline development that is grossly normal until the L4 larval stage followed by strong germline atrophy was reminiscent of a germline degeneration phenotype that was proposed to occur when *C. elegans* L4 larvae are starved, some of which emerge as adults that are in a stress-resistant state of reproductive quiescence known as ARD (Angelo and Van Gilst, 2009). The apoptosis gene *ced-3* and the nuclear hormone receptor *nhr-49*, which is an NHF4-alpha homolog responsible for mediating fatty acid oxidation and gluconeogenesis during starvation (Van Gilst et al., 2005a, 2005b), promoted germline remodeling in starvation-induced ARD (Angelo and Van Gilst, 2009). We found that *ced-3* and *ced-4* mutations, which eliminate apoptotic cell death (Metzstein et al., 1998), led to a significant change to the germline profiles of day 1 sterile *prg-1* mutant adults (Table S1), and overall reduced levels of germline atrophy, as did deficiency for *nhr-49* (Figure 1D). Thus, the sterility of late-generation *prg-1* mutants is accompanied by a germ cell atrophy phenotype that requires the genetic constituents of starvation-induced ARD.

Mammalian p53 as well as the *C. elegans* homolog of p53, CEP-1, can promote apoptosis or cell cycle arrest in response to DNA damage, heat shock, anoxia, and oxidative or osmotic stresses (Gartner et al., 2008). The germline profile of sterile *prg-1 cep-1* double mutant day 1 adults was significantly altered (Figure 1D; Table S1), with germline atrophy being strongly inhibited but not abolished. Sterile *prg-1 cep-1* double mutants became fertile on day 2 through day 5, similar to *prg-1* single mutants (Figure 5A), indicating that germ cell atrophy is not required for delayed fertility of late-generation *prg-1* mutants. In starvation-induced ARD, mutation to *ced-3* did not impair ARD entry, but the reduction in germ cell number was impaired and, upon addition of food, the level of ARD exit dropped significantly but was not eliminated (Angelo and Van Gilst, 2009). We constructed *prg-1 cep-1; ced-3* and *prg-1 cep-1; ced-4* triple mutants, which are deficient for both CEP-1/p53 and core apoptosis genes. *prg-1 cep-1; ced-4* had a similar percentage of atrophied germlines in comparison to *prg-1 cep-1* and *prg-1; ced-4* controls, although their germline profiles were significantly different (Figure 1D; Table S1). *prg-1 cep-1; ced-3* triple mutants displayed the lowest level of germ cell atrophy and the strongest return

Figure 2. Germline Atrophy in Sterile *prg-1* Animals

(A–O) DAPI-stained photos of (A) N2 wild-type L4, (B) sterile-generation *prg-1* L4, (C) N2 wild-type adult, (D) fertile *prg-1* mutant, (E and F) short germline from sterile adult *prg-1* mutants, (G and H) atrophied germlines from sterile adult *prg-1* mutants, (I) empty germline from sterile adult *prg-1* mutant lacking germ cells, (J) distal mitotic region of a fertile N2 wild-type adult, (K) meiotic region of a fertile N2 adult containing a transition zone where chromosomes pair during initiation of meiosis as well as meiotic pachytene cells undergoing homologous recombination, (L) arrested cells in an atrophied germline of a sterile adult *prg-1* mutant, (M) distal region of a short germline in a sterile adult *prg-1* mutant, (N) meiotic cells near the germline bend in a short germline from a sterile *prg-1* adult, and (O) meiotic cells in a sterile *prg-1 daf-16* adult. Dashed lines indicate germline. Scale bars, 50 μm in (A–I) and 10 μm in (J–O). (J) and (L) show examples of mitotic cells, and (K) and (O) arrows show examples of meiotic cells.

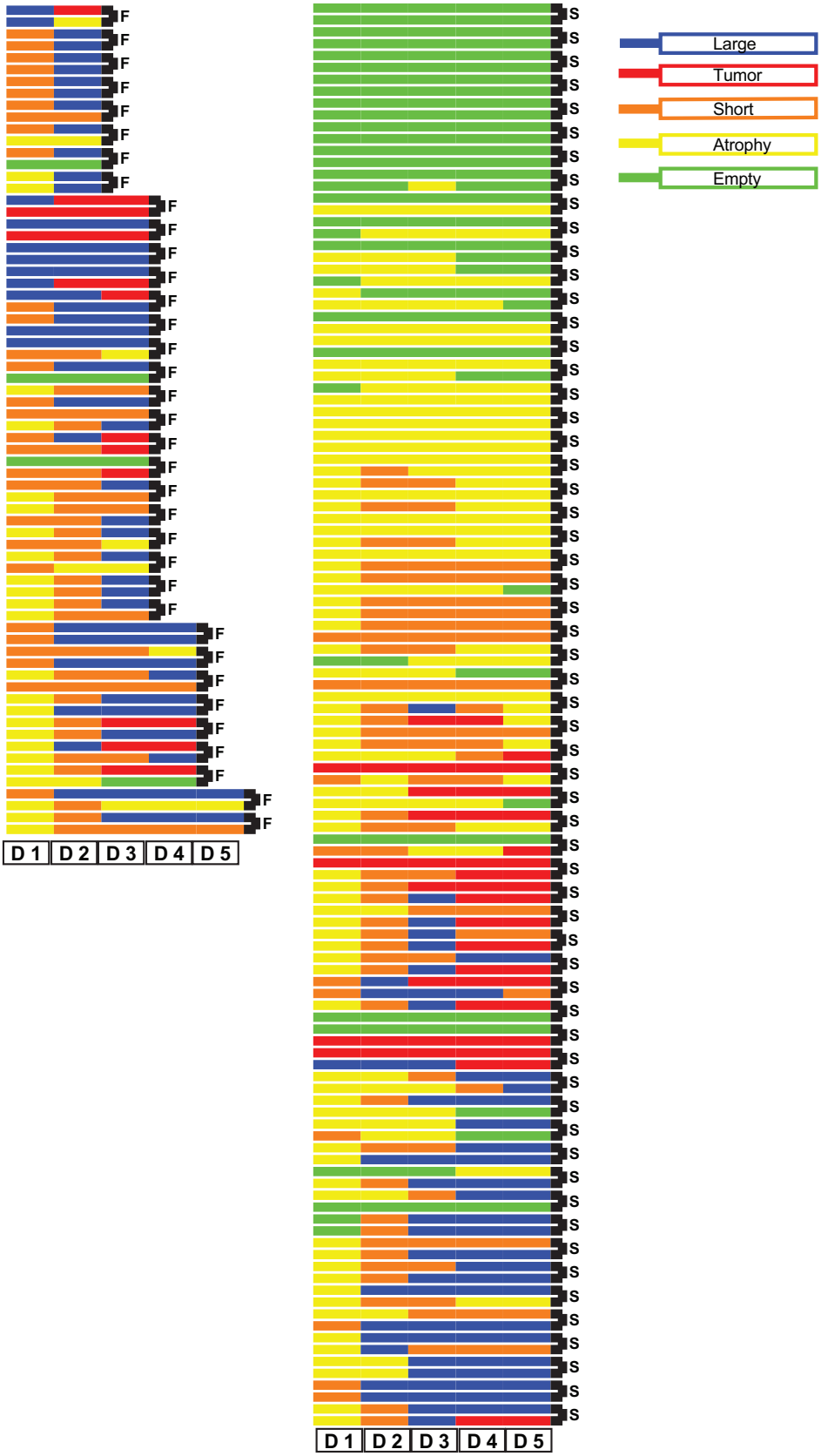

(legend on next page)

of large germlines of any strain tested, whereas *prg-1 cep-1; ced-4* triple mutants generally displayed short rather than large germline arms (Figures 1D and 5C). The simplest interpretation of the *cep-1* and *ced* double- and triple-mutant data is that CEP-1 functions in the classical apoptosis pathway to promote germ cell atrophy in sterile *prg-1* animals (Schumacher et al., 2001). The short germlines observed in *prg-1 cep-1; ced-4* triple mutants could reflect a caspase-independent function of CED-4, for example as previously shown for regulation of cell size (Chen et al., 2008).

Apoptotic corpses occur in the pachytene region of the adult *C. elegans* germline and can be visualized as discrete rings using GFP-tagged CED-1, a transmembrane protein that promotes engulfment of apoptotic corpses (Zhou et al., 2001). Consistently, we observed apoptotic corpses in adult wild-type control germlines (Figure 4A), but CED-1::GFP activity was not observed for wild-type L4 larvae (Figures 4D, 4G, and 4J). We constructed *prg-1; ced-1::GFP* strains and observed that day 1 adult early-generation (F4), late-generation, and sterile-generation 1-day-old adults displayed elevated apoptotic corpses with a trend toward increased occurrence in later generations (Figures 4B, 4C, and 4M), consistent with the concept that transposon-induced DNA damage may promote the fertility defect of *prg-1* mutants (McMurchy et al., 2017). Sterile-generation but not early-generation *prg-1* mutant L4 larvae displayed pronounced CED-1::GFP activity in both proximal and distal regions of the germline (Figures 4E, 4F, 4H, 4I, 4K, and 4L). A developmental time course of sterile-generation L4 larvae revealed strong CED-1::GFP activity in germlines of mid-L4 larvae (Figures 4I and 4N). Together, our data imply that an apoptotic program can act throughout the germline of L4 larvae to promote germ cell atrophy as sterile-generation *prg-1* mutants mature into day 1 adults.

Germ cell atrophy still occurred for some sterile-generation *prg-1* mutant adults that were deficient for the core cell death proteins *ced-3* or *ced-4* (Figure 1D). We asked whether necrotic cell death contributed to germ cell atrophy by inactivating the *C. elegans* calreticulin ortholog *crt-1* (Syntichaki et al., 2002). Sterile-generation *prg-1; crt-1* double mutants displayed reduced levels of germ cell atrophy, and a significant change to their germline profile (Figure 5C; Table S1). We constructed *prg-1 cep-1; crt-1* triple mutants to eliminate both necrosis and apoptosis. This resulted in a significant change in the germline profile compared to *prg-1 cep-1* (Figure 5C; Table S1) but surprisingly failed to remove the germ cell atrophy phenotype. However, an increased frequency of germ cell tumors was observed (Figure 5C). These results imply that CEP-1/p53 promotes germ cell atrophy by activating necrotic cell death, which is consistent with an established role for Mammalian p53 in promoting necrotic cell death (Baumann, 2012). However, the increase in germ cell tumors for *prg-1; crt-1* double mutants and a further increase for *prg-1 cep-1; crt-1* triple mutants, suggests a non-redundant role for CEP-1/p53 and the necrotic cell factor CRT-1 in suppression of germ cell tumor formation.

Insulin/IGF1 Signaling Promotes Germ Cell Atrophy in Sterile *prg-1* Mutants

The *C. elegans* DAF-16/Foxo transcription factor can promote resistance to diverse stresses including starvation, heat shock, proteotoxicity, oxygen radicals, pathogenic bacteria, and high metal concentrations (Zhou et al., 2011), and even promotes germline apoptosis in a manner that can repress germ cell tumors (Pinkston-Gosse and Kenyon, 2007). We found that sterile late-generation *prg-1 daf-16* double-mutant day 1 adults had a significant change in their germline profile compared to day 1 sterile *prg-1* mutant adults (Figure 1D; Table S1), with strongly reduced frequencies of germline atrophy. In agreement with these data, when *prg-1 daf-16; daf-2* mutants were analyzed for their germline profiles there was a strong reduction in germline atrophy and a profile that was similar overall to that of *prg-1 daf-16* double mutants (Figure S1F). This demonstrates that *daf-2* mutation does not rescue the germline phenotypes of *prg-1 daf-16* double mutants back to wild-type or otherwise alter them. Strongly reduced frequencies of germline atrophy were also observed in sterile late-generation day 2 and day 3 *prg-1 daf-16* double-mutant adults (Figure 5B), which instead possessed an increased number of "short" germline arms that displayed hallmarks of normal meiosis including a transition zone and synapsed homologous chromosomes (Dernburg et al., 1998), as well as mature oocytes at the proximal end of the germline (Figures 1D, 2O, and S2G). DAF-16 can function downstream of *C. elegans* PTEN tumor suppressor homolog DAF-18 to promote longevity in response to reduced DAF-2 signaling but can also respond to distinct signals from other pathways (Ogg and Ruvkun, 1998; Vowels and Thomas, 1992). We found that sterile late-generation *prg-1; daf-18* double-mutant day 1 adults had a significant change in their germline profiles (Table S1) and displayed reduced germ cell atrophy and an increased frequency of short germlines with differentiated germ cells, in comparison to *prg-1* single-mutant controls (Figure 1D). While it is possible that these genes could function in parallel pathways, we suggest that DAF-16/FOXO functions downstream of DAF-18/PTEN to promote germline remodeling in late-generation *prg-1* mutant L4 larvae that are poised to become sterile, and suggest that DAF-16 responds to reduced *daf-2* insulin/IGF1-signaling cues in this context.

DAF-16 interacts with the heat shock transcription factor HSF-1 to promote longevity (Hsu et al., 2003). DAF-16 and HSF-1 can respond to common forms of stress, and they influence the expression of common transcriptional targets (Hsu et al., 2003). Sterile day 1 *prg-1 hsf-1* double-mutant adults displayed reduced germline atrophy and an increase in small germlines at frequencies similar to *prg-1 daf-16* double mutants,

Figure 3. Regrowth of Sterile Germline Arms

Anterior (top of pair) and posterior (bottom of pair indicated with black connector bar) germline arms in day 1 sterile *prg-1; cpls36* were blindly scored live daily for germline phenotype along with the presence of F1 progeny. Each sequential block represents a score for particular day, and the color indicates the germline phenotype observed. Each gonad arm was tracked daily until fertility returned (F, fertile; left column) or remained completely sterile for 5 days (S, sterile; right column). In many cases, only one gonad arm regained fertility while the other remained sterile, such that embryos were observed only on one side of the uterus or the other germline arm remained in state of atrophy or empty.

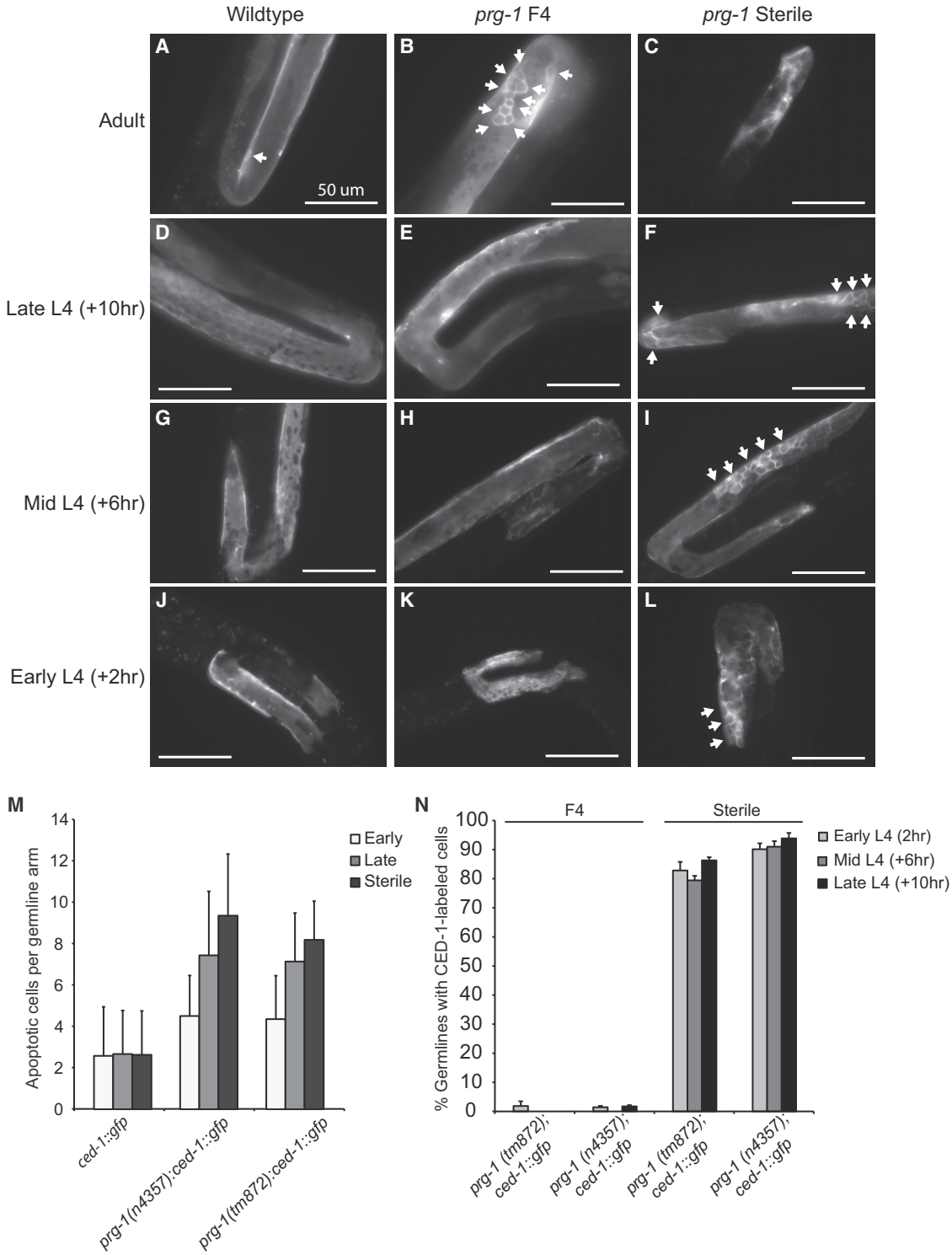

Figure 4. Increased Apoptosis in Early- and Late-Generation *prg-1* Animals

(A and B) Compared to wild-type (A), *prg-1* animals (B) display and increase number of apoptotic cells, indicated by white arrows.

(C) Sterile-generation animals with atrophied germline.

(D, G, and J) Wild-type L4 germlines observed at early (L4 0 hr) (J), mid (L4 +4 hr) (G), and late (L4 +8 hr) (D) time courses.

(E, H, and K) Fertile, early-generation *prg-1* L4 germlines observed at early (L4 0 hr) (K), mid (L4 +4 hr) (H), and late (L4 +8 hr) (E) time courses.

(legend continued on next page)

resulting in no significant difference between their germline profiles (Figure 1D; Table S1). This suggests that HSF-1 and DAF-16 interact to promote germ cell atrophy in sterile *prg-1* adults.

To investigate the relationship between CEP-1/CED-3/CED-4 apoptosis and DAF-16/DAF-18/HSF-1/NHR-49 stress response pathways (Kenyon, 2010; Metzstein et al., 1998; Ratnappan et al., 2014), we generated triple mutants involving *prg-1*, apoptosis, and longevity mutations. *prg-1 daf-16; ced-4* mutants and *prg-1 nhr-49; ced-4* mutants both favored short rather than large germline arms, comparable to *prg-1 daf-16* and *prg-1 nhr-49* double mutants at day 1 (Figure 1D). Furthermore, when comparing their germline profiles, they were either weakly significant or not significantly different (Table S1). The lack of additivity observed for these triple mutants, in terms of a further reduction of germ cell atrophy on day 1 of adulthood, suggests that these genes act in a single pathway to promote germ cell atrophy in sterile *prg-1* mutants.

prg-1 Mutant Sterility Is a Reversible State of Reproductive Quiescence

For starvation-induced ARD, addition of food can restore fertility to a small fraction of sterile animals, demonstrating that ARD is a facultative stress response that suspends reproduction in response to starvation until favorable nutritional cues are encountered (Angelo and Van Gilst, 2009). We previously found that reduced *daf-2* signaling can abolish the progressive sterility phenotype of *prg-1* mutants (Simon et al., 2014). Consistently, when we removed *daf-2* from early-generation *prg-1* mutants, this resulted in robust fertility for many generations (Figure 6B). We also asked whether a *daf-2* mutation could rescue the progressive sterility of late-generation *prg-1* mutants by propagating sibling strains that were heterozygous for a recessive *daf-2* mutation but homozygous mutant for *prg-1* until late generations (F18) and then isolated *prg-1* −/−; *daf-2* −/− homozygotes. However, mutation of *daf-2* failed to ameliorate the fertility defect of late-generation *prg-1* mutants. In parallel, we asked whether RNAi knockdown of *daf-2* in fertile late-generation *prg-1* mutants would ameliorate the very low levels of fertility that they experience prior to the onset of sterility. However, *daf-2* RNAi failed to improve the weak fecundity of fertile late-generation *prg-1* mutants (Figure 6A).

As a negative control, we next asked whether sterile *prg-1* adults would remain sterile when *daf-2* signaling is reduced. Wild-type worms can reproduce until day 8 of adulthood (Hughes et al., 2007), so we identified 10-day-old sterile *prg-1* adults with atrophied germlines and surprisingly found that a small but significant population became fertile upon treatment with *daf-2* RNAi (Figure S1C). We next re-tested these results under our present laboratory conditions for *prg-1* mutant animals that were sterile through day 5 of adulthood. These animals remained sterile on nematode growth medium (NGM) plates with standard OP50 bacteria (Figure 1A), but fertility was restored to a small yet significant fraction of animals placed on RNAi plates seeded with HT115 bacteria expressing double-stranded RNA (dsRNA) targeting *daf-2* or *gfp* and also for the L4440 empty vector RNAi control (Figure 5D). Additionally, crossing day 7 sterile *prg-1* mutant adults that were transferred to RNAi plates with wild-type males did not markedly improve the rescue from sterility (Figure S1E). Furthermore, treatment of HT115 bacteria expressing dsRNA for L4440 empty vector or *daf-2* did not enhance the restoration of fertility for late-generation sterile day 2 *prg-1* mutants (Figure S1D). We next asked whether HT115 *E. coli* used for RNAi feeding was responsible for this effect, but found that RNAi plates seeded with OP50 *E. coli* that lack an antibiotic resistance plasmid resulted in restoration of fertility to sterile *prg-1* mutant adults (Figure 5E). These results imply that the sterility of 5-day-old sterile *prg-1* adults represents a state of reversible reproductive diapause. We conclude that bacteria grown on RNAi plates can reverse the sterility of a fraction of sterile *prg-1* mutants. We tried restoring fertility to day 5 *prg-1* mutant adults using bacteria grown on plates containing single compounds found in RNAi plates, which contain ampicillin, tetracycline, and isopropyl β-D-1-thiogalactopyranoside (IPTG) but found that no single compound was sufficient to restore fertility (Figure 6G). These results also indicate that deficiency for *daf-2*, either by RNAi or by mutation, does not specifically suppress the fertility defects of late-generation *prg-1* mutants.

A DAF-16-Mediated Small RNA Pathway Promotes Fertility of Sterile *prg-1* Adults

DAF-16 is a FOXO transcription factor that acts downstream of the insulin/IGF1-like receptor *daf-2* and is required for the immortality of *prg-1 daf-2* double mutants (Simon et al., 2014). When we passaged *prg-1 daf-16* double mutants until the sterile generation, we found that similar to the *prg-1* single mutants, 23% of *prg-1 daf-16* double-mutant worms that were sterile on day 1 became fertile on day 2. Likewise, 18% of sterile day 2 adults, 13% of sterile day 3 adults, and 2% of sterile day 4 adults became fertile (Figure 6C). However, no *prg-1 daf-16* adults that were sterile through day 5 exited ARD to become fertile when placed on RNAi plates seeded with HT115 bacteria (Figure 6E). As mutation of *daf-16* suppressed germ cell atrophy in sterile *prg-1* mutants (Figure 1D), we asked whether *cep-1*, mutation of which more strongly suppressed *prg-1* mutant germ cell atrophy (Figures 1D and 5C), affected the restoration of fertility to sterile 5-day-old *prg-1* mutants. However, *cep-1* was not required for ARD exit (Figure 6E).

Constitutive activation of DAF-16 in early-generation *prg-1* mutants indefinitely promotes the fertility of *prg-1* mutants by activating an endogenous small RNAi silencing pathway that depends on *mut-7*, which promotes secondary small interfering RNA (siRNA) biogenesis (Simon et al., 2014). We therefore asked whether MUT-7 might function downstream of DAF-16

(F, I, and L) Sterile-generation *prg-1* L4 germlines observed at early (L4 0 hr) (L), mid (L4 +4 hr) (I), and late (L4 +8 hr) (F) time courses, indicating an increase in the number of apoptotic cells.
(M) Average number of apoptotic cells in early-generation adult germlines (n > 30 for all samples).
(N) Sterile-generation animals displayed CED-1::GFP activity throughout L4 germline development. Arrows indicate apoptotic cells. Error bars indicate SEM.

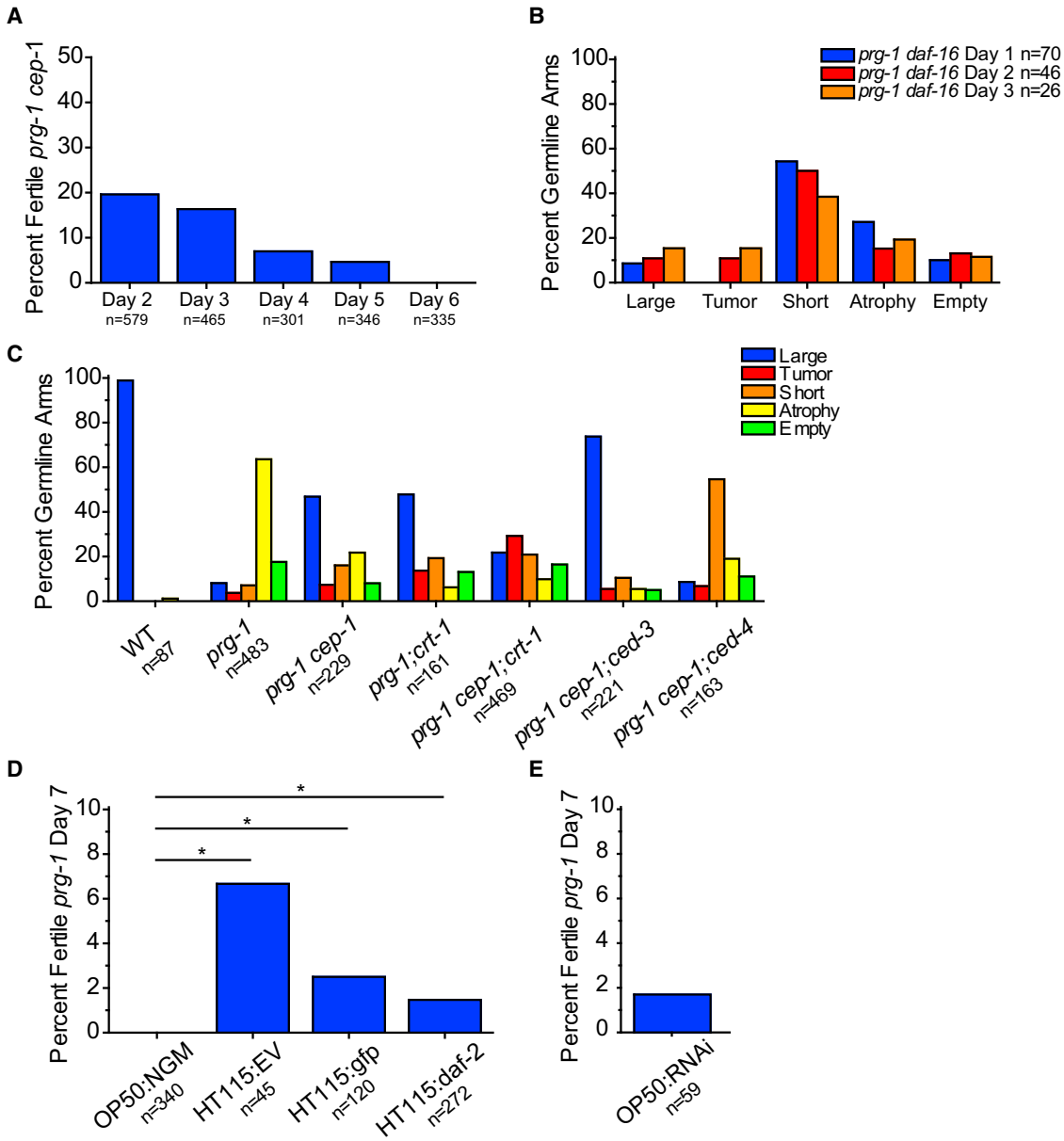

Figure 5. *prg-1* Germline Arm Phenotypes and Sterility Can Be Suppressed

(A) Sterile day 1 *prg-1(n4357) cep-1(gk138)* animals were scored for continued sterility from days 2 through 6. n represents total worms scored on that day that were previously sterile.

(B) Germline phenotypes of sterile germlines in day 1, day 2, and day 3 *prg-1 daf-16* mutants.

(C) Effects of apoptosis and necrotic cell death pathways on sterile germline phenotypes of *prg-1*. For comparison, we include wild-type, *prg-1*, and *prg-1 cep-1* data that are the same data as shown in Figure 1D. p values were determined using pairwise chi-square tests with Bonferroni correction that can be found in Table S1.

(D) Sterile day 5 *prg-1* mutants on either standard laboratory plate NGM plates with OP50 *E. coli* (OP50:NGM) or on RNAi plates seeded with various bacteria relevant to generating dsRNA (HT115:RNAi clone; EV is empty vector) scored for percent fertility 48 hr after treatment (day 7) *$p < 0.05$, Fisher's exact test with Bonferroni correction.

(E) Sterile day 5 *prg-1* mutants on OP50 bacteria on standard RNAi plate condition (OP50:RNAi) scored for percent fertility 48 hr after treatment (day 7). Data combined from minimum of three independent experiments; n represents total worms (A, D, and E) or germline arms (B and C) scored.

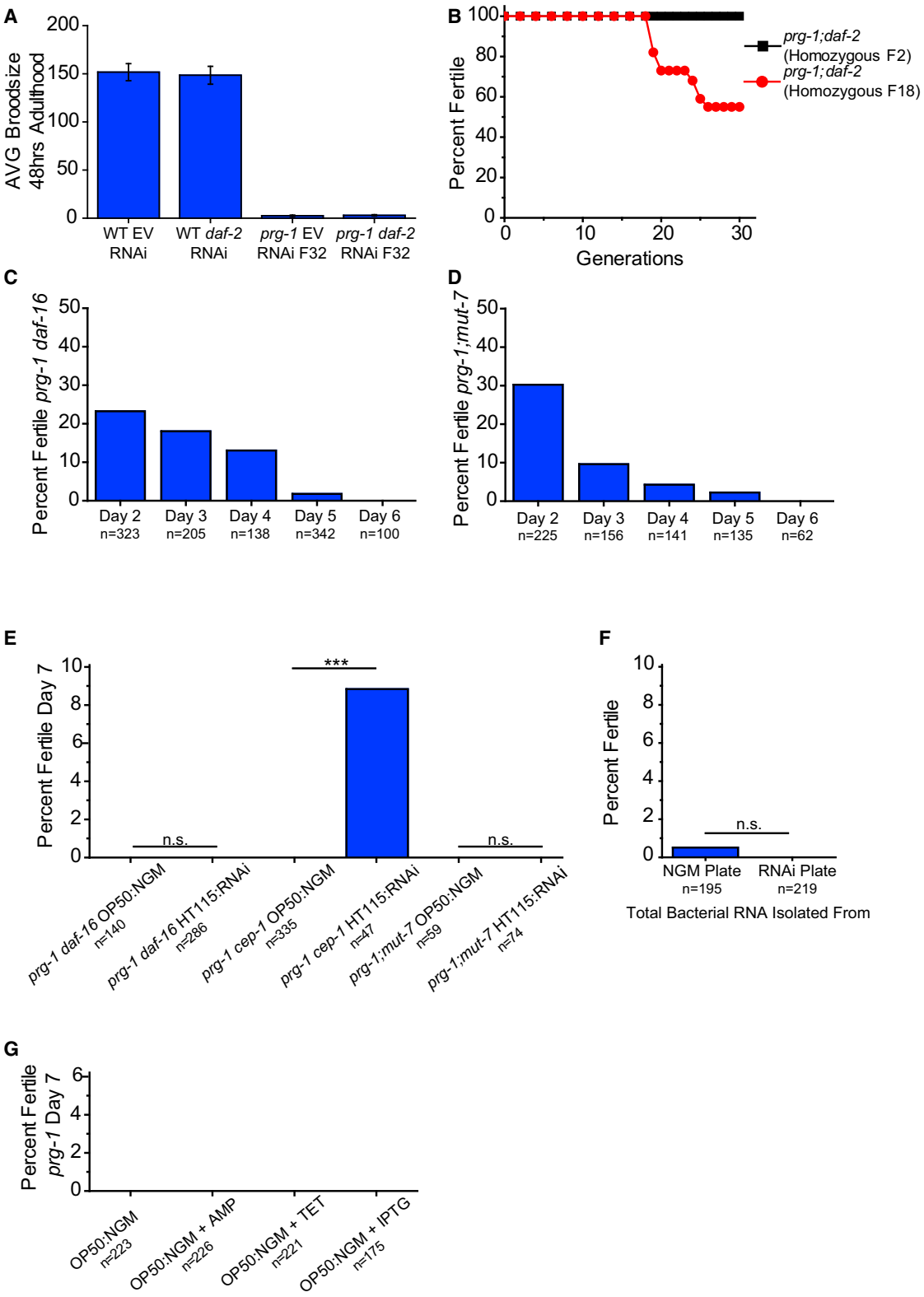

Figure 6. Insulin Signaling and Downstream Small RNA Pathway Are Necessary for Reversal of *prg-1*-Induced ARD

(A) Average brood size of day 2 wild-type worms or fertile, late-generation *prg-1* mutants on empty vector (EV) or RNAi clone targeting *daf-2*. Error bars indicate SEM.

(legend continued on next page)

in reversing the sterility of 5-day-old sterile *prg-1* mutants. Although significant fractions of sterile *prg-1; mut-7* day 1 double mutants became fertile on days 2–5, we found that no 5-day-old sterile *prg-1; mut-7* double-mutant adults became fertile when placed on *E. coli* grown on RNAi plates (Figures 6D and 6E). This indicates that MUT-7 and a small RNAi silencing pathway downstream of DAF-16 are required for exit of *prg-1*-induced ARD but are not required for spontaneous reversal of fertility that occurs on days 2–5.

As MUT-7 promotes secondary siRNA biogenesis and therefore promotes many types of small RNA responses in *C. elegans*, we asked whether RNA generated by bacteria grown on RNAi plates might be responsible for restoring fertility to sterile late-generation *prg-1* mutants. Total RNA was isolated from bacteria grown on NGM or RNAi plates and was either injected or soaked into sterile day 5 *prg-1* mutant adults. However, RNA from bacteria grown on RNAi plates failed to specifically restore fertility to sterile 5-day-old *prg-1* mutant adults (Figure 6F). Taken together, these results suggest that *E. coli* grown on RNAi plates but not RNA from these *E. coli* cells can activate a DAF-16-mediated endogenous RNAi pathway that can restore fertility to a small fraction of sterile *prg-1* mutant adults. Together, our results indicate that although activation of DAF-16 was not capable of suppressing the fertility defect of late-generation *prg-1* mutants (Figure 6A), that activation of DAF-16 in early generations abolishes the *prg-1* mutant fertility defect (Figure 6B) (Simon et al., 2014) and that an endogenous DAF-16-mediated RNAi pathway can restore fertility to sterile 5-day-old *prg-1* mutant adults in response to bacteria grown on RNAi plates.

DISCUSSION

Here, we demonstrate that sterile-generation *prg-1* mutants activate two mechanisms to delay fertility. The first mechanism delays fertility from 1 to 4 days (Figure 1) and involves a large-scale germ cell apoptotic program during the final larval stage (Figures 1 and 4). On day 1 of sterility, the majority of germlines were atrophied (Figures 1 and 3). Germline regrowth can occur for day 2, 3, and 4 adults, accompanied by restoration of fertility for some animals (Figures 1 and 3). Defects in insulin signaling and cell death pathways suppressed but did not eliminate germ cell atrophy (Figures 1 and 5). Apoptosis, insulin signaling pathways, and necrosis pathways appear to function in a single pathway to promotes germ cell atrophy whose wiring remains to be elucidated (Figure 7). Although germ cell atrophy is a pronounced feature of the delayed fertility mechanism that we describe, it is not necessary for it.

prg-1 mutant animals that remained sterile until day 5 of adulthood revealed a second mechanism to delay fertility, where they can remain sterile indefinitely but can become fertile if provided with a cue from a food source (Figure 5). This second response of *prg-1* mutants to delay reproduction represents a form of ARD (Roy et al., 2016; Seidel and Kimble, 2011, 2015). Thus, sterile-generation *prg-1* mutants undergo a dynamic form of ARD that delays sterility in two ways: first, by delaying the onset of fertility for 1–4 days, a phenotype that may be masked by the highly crowded conditions of starvation-induced ARD (Angelo and Van Gilst, 2009), and second by inducing a form of reproductive quiescence in day 5 adults that can be reversed when an alternative food source is provided.

Given this parallel with starvation-induced ARD, we propose that germ cells of *prg-1* mutants transmit an escalating form of ''heritable stress'' that ultimately becomes comparable to severe environmental stresses such as starvation (Figure 7). A heritable stress that can be transmitted by gametes could be broadly relevant to the concept of inheritance and related epigenetic phenomena, and possibly to human adult-onset disorders that are affected by exogenous stresses. The delayed fertility and reproductive quiescence responses of sterile-generation *prg-1* adults reflect a dynamic developmental program that delays fertility in a non-uniform manner in populations of sterile-generation *prg-1* mutant adults, which may represent a concerted effort to outlast or adapt to the heritable stress prior to reproduction. Loss of Piwi in *Drosophila*, zebrafish, and mice results in immediate sterility that correlates with transposon-induced genome instability (Juliano et al., 2011), and expression of the Mirage transposon has been demonstrated to contribute to the fertility defects of late-generation *prg-1* mutants (McMurchy et al., 2017). Our results suggest that the sterility of Piwi mutants in other species could be due to an epigenetic stress response that immediately triggers ARD. If so, it might be possible to restore fertility to these Piwi mutants.

What is the nature of this heritable stress? We considered that homologous recombination defects might promote sterility. Sterile *prg-1* mutants at 20°C displayed six DAPI bodies in their oocytes (Simon et al., 2014), which correspond to homologous chromosomes that are held together by recombination crossovers. Small RNA mutants that become sterile only if grown at 25°C show an increase in these DAPI bodies (Sakaguchi et al., 2014); we examined sterile *prg-1* mutants that were grown at 25°C but these did not show more than six DAPI bodies in their

(B) Mortality assay for 30 generations of *prg-1; daf-2* mutants homozygous at F2 and *prg-1; daf-2* mutants that were made homozygous for *daf-2* at F18.
(C) Sterile day 1 *prg-1(n4357) daf-16* animals were scored for continued sterility from days 2 through 6. n represents total worms scored on that day that were previously sterile.
(D) Sterile day 1 *prg-1(n4357) mut-7 (pk204)* animals were scored for continued sterility from days 2 through 6. n represents total worms scored on that day that were previously sterile.
(E) Sterile day 5 *prg-1 daf-16* or *prg-1 cep-1* or *prg-1; mut-7* mutants on either standard laboratory NGM plates seeded with OP50 *E. coli* (OP50:NGM) or standard RNAi plates seeded with HT115 *E. coli* (HT115:RNAi) scored for percent fertility 48 hr after treatment (day 7). ***$p < 0.0001$, Fisher's exact test.
(F) Sterile day 5 *prg-1* mutants were treated with total RNA isolated from bacteria on standard laboratory plate conditions (NGM) or standard RNAi plate conditions (RNAi) and scored for fertility. p = n.s., Fisher's exact test.
(G) Percent fertile sterile day 5 *prg-1* mutants on either standard OP50:NGM plate conditions or OP50:NGM with ampicillin (AMP) or tetracycline (TET) or IPTG. Above data combined from minimum of three independent experiments; n represents total worms scored.

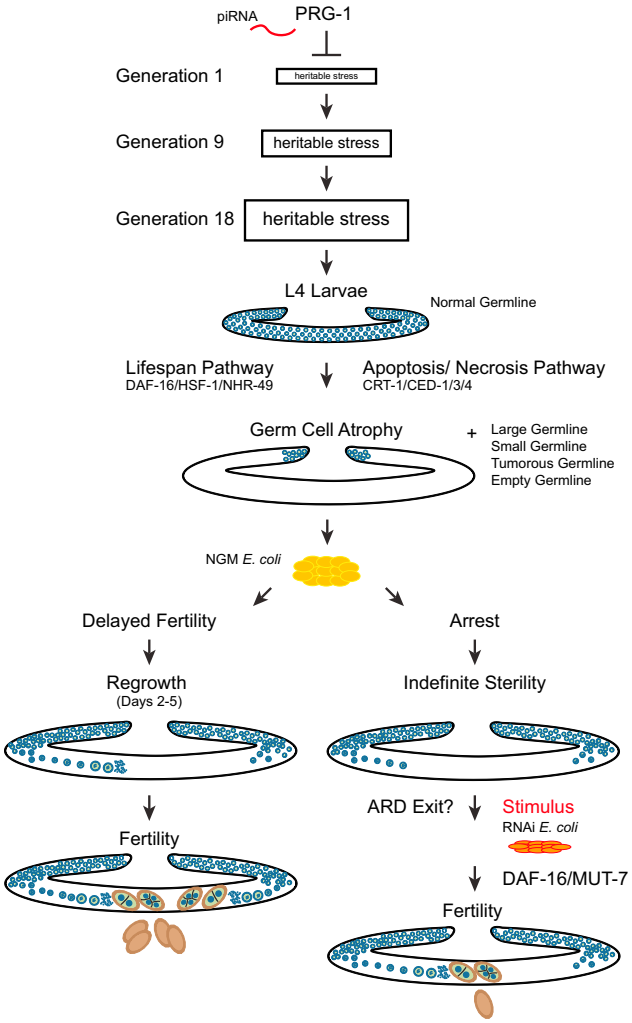

Figure 7. Model of PRG-1

PRG-1 suppresses a heritable form of stress that triggers adult germ cell remodeling and drives a form of arrest. Delayed fertility pathway (left) is *prg-1* mutants that spontaneously reverse from loss of fertility to fertile state. Reproductive diapause pathway (right) is *prg-1* mutants that remain sterile throughout adulthood and only return to fertility when given an undetermined stimulus. Blue represents germ cells. Brown represents embryos.

oocytes (Figure S1G). This implies that homologous recombination is nominally fine in sterile *prg-1* mutants, although minor meiotic or mitotic chromosome segregations defects may occur, as a weakly penetrant X chromosome loss phenotype is observed in mid- and late-generation *prg-1* mutant strains. Previous work revealed that immediate sterility occurred if *prg-1*/piRNA mutants that are devoid of secondary siRNAs are crossed in a manner that restores secondary siRNAs but leaves *prg-1* mutant (de Albuquerque et al., 2015; Phillips et al., 2015). In this scenario, Ketting and colleagues observed that sterile *prg-1* mutants displayed a range of adult germline phenotypes that are consistent with those that we observed for *prg-1* single mutants after many generations of growth. The sterility observed by the Ketting and Ruvkun groups, which was attributed to secondary siRNA dysfunction in the context of the pro- and anti-small RNA silencing pathways of *C. elegans*, could be relevant to the sterility in *prg-1* mutants.

We previously suggested that desilencing of repetitive segments of the genome may explain the sterility phenotype of *prg-1* mutants (Simon et al., 2014). Two recent studies support this possibility, as acute desilencing of heterochromatin and perturbation of a variety of genes that promote heterochromatin formation can elicit fertility defects that are consistent with a form of DNA damage evoked by desilencing of heterochromatin (McMurchy et al., 2017; Zeller et al., 2016). Consistently, the Kennedy group recently identified additional *mortal germline* mutants that are defective for RNA inheritance and likely become sterile due to epigenetic deregulation in germ cells (Spracklin et al., 2017).

Transgenerational fertility defects that result in heterochromatin dysfunction may provide insight into forms of stress that accumulate as human somatic cells proliferate during aging and senesce. Links between aging and the epigenome have been noted, such as desilencing of retrotransposons in senescent human cells, and epigenetic silencing of retrotransposons by the anti-aging protein SIRT6 in the mouse (De Cecco et al., 2013; Gorbunova et al., 2014; Van Meter et al., 2014). Moreover, repetitive elements play major roles in genome evolution. For example, rapid evolution of tandem repeats that specify vertebrate centromeres promotes genomic conflict and speciation (Malik and Henikoff, 2002). Given that harsh environmental conditions can trigger ARD (Angelo and Van Gilst, 2009; Ragland et al., 2010), we propose that ARD can also occur in response to endogenous epigenetic stress, such as that encountered in the context of genomic conflict, or when transposons or retroviruses enter the germline in horizontal transfer events and create bursts of genomic stress. Perinuclear P granules, or germ granules, that contain components of anti-viral and anti-transposon response systems may represent a focal point for the interface between epigenomic regulation and germ cell development (Strome and Updike, 2015).

When starvation-induced ARD worms are returned to food, a small percentage of worms are able to regrow their germlines and become fertile again (Angelo and Van Gilst, 2009). We observed a similar reproductive quiescence phenotype in sterile 5-day-old *prg-1* mutant adults, a small percentage of which can respond to a signal from bacteria grown on RNAi plates to exit reproductive diapause. Although DAF-16 played a less pronounced role in germ cell atrophy than CEP-1/p53, we found that DAF-16 and MUT-7, which promotes a DAF-16-dependent small RNA-mediated genomic silencing pathway that can eliminate the transgenerational fertility defect of *prg-1* mutants, but not *cep-1*/p53, were required for ARD exit of day 5 *prg-1* mutant adults in reproductive diapause. Further insight into the restoration of fertility to sterile *prg-1* mutants is an important future goal, but one that may be technically challenging given the low frequency of such events. Given that HSF-1 and DAF-16 can act at the same promoters in the context of longevity (Hsu et al., 2003), it is plausible that CEP-1/p53 shares transcriptional targets with these proteins, or that insulin signaling in the soma could function upstream of cell death/necrosis in the germline. We suggest that the DAF-16 stress response transcription factor

plays distinct roles in responding to a heritable stress transmitted by *prg-1* mutants, where it promotes germ cell atrophy in L4 larvae and ARD exit for day 5 sterile worms. For ARD exit, DAF-16 and the small RNA pathway protein MUT-7 are likely to promote an epigenomic silencing process that is capable of restoring fertility to *prg-1* mutants (Simon et al., 2014).

We conclude that ARD may represent a biological checkpoint that can integrate development with genome evolution, transiently suspending reproduction until the germ cells of an organism can respond or adapt to a genomic incident. Environmental stress has the potential to induce either ARD (Angelo and Van Gilst, 2009; Ragland et al., 2010) or Lamarckian inheritance (Choi and Mango, 2014), and our data suggest that *Piwi/prg-1* mutants may transmit a form of heritable stress that may accumulate to engage the ARD stress response. Our study therefore suggests a possible interface between heritable and environmental forms of stress, which in conjunction with ARD could represent a cornerstone of the evolutionary biology of aging in metazoans. Our study lays the foundation for future work to investigate how cell death, insulin signaling, and small RNA pathways interface with germline development to modulate germ cell immortality and ARD.

EXPERIMENTAL PROCEDURES

Strains

Unless noted otherwise, all strains were cultured at 20°C on NGM plates seeded with *E. coli* OP50. Strains used are listed in Supplemental Experimental Procedures.

prg-1 mutations were outcrossed versus an outcrossed stock of *dpy-5(e61) unc-13(e450)*, and freshly isolated homozygous F2 lines were established for analysis. *dpy-5 unc-55; daf-2* triple mutants were crossed with *prg-1/dpy-5(e61) unc-13(e450)* males, which were then selected based on a Dauer phenotype at 25°C and on loss of *dpy-5 unc-55* to create *prg-1; daf-2*. Analogous crosses using marker mutations *dpy-17* for *ced-4*, or *dpy-9* for *daf-18*, or *unc-24* for *ced-3*, as balancers to create double-mutant strains. To create the linked *prg-1 daf-16* double mutant, *prg-1 dpy-24* and *unc-13 daf-16* double mutants were first created, and then progeny of *prg-1 dpy-24/unc-13 daf-16* heterozygotes that lost *unc-13* were identified, and the resulting putative *prg-1 daf-16* recombinant chromosomes were made homozygous and PCR genotyped to verify the presence of *prg-1* or *daf-16* deletions. *prg-1 daf-16* double mutants were crossed with *unc-13 dpy-24; daf-2* / + +; + heterozygous males and then selected for Daf and against Dpy Unc phenotypes to create *prg-1 daf-16; daf-2* triples.

Sterility Assays

Due to the heterogeneity of the Mortal Germline phenotype (Mrt) in the *prg-1* population, it is technically difficult to obtain large populations of sterile late-generation animals. *prg-1* worms were grown by transferring six L1s to fresh NGM plates every other generation until small brood sizes were observed in later generations, and then many individual animals were singled and scored for sterility. At L4 (day 0), individual worms were tracked for sterility and scored each day for the presence of progeny. In brood size assays, total progeny were counted.

Germline Mortality Assay

Worms were assessed for the Mrt phenotype using the assay previously described (Ahmed and Hodgkin, 2000). L1 or L2 larvae were transferred for all assays.

Germline Visualization

DAPI staining was performed as previously described (Ahmed and Hodgkin, 2000). L4 larvae were selected from sibling plates, and sterile adults were singled as late L4s and observed every 24 hr to monitor sterility. Sterile worms were stained, and each germline arm scored using immunofluorescence on Nikon Eclipse E800 microscope using NIS Elements software. Germline arms were qualitatively characterized into five categories based on comparisons to wild-type (WT) controls. Large germlines contained both mitotic and meiotic cells, a bend in the gonad arm, and overall size and architecture comparable to a wild-type worm. Tumorous germlines resembled proximal proliferative tumors (Korta et al., 2012). Short germlines were characterized as germline arms that had both mitotic and meiotic cells, typically a bend in the gonad arm, but were far shorter and under proliferated compared to both large germlines and wild-type controls. Atrophy germlines were characterized as a small population of germ cells (50–100) near the distal tip cell that were typically uniformly mitotic and devoid of meiotic germ cells. Empty germlines were devoid of all or almost all germ cells.

cpIs36 was crossed into *prg-1* mutants and used to visualize the germline in live animals. Germlines were blindly qualitatively scored by eye, comparing size and architecture to *cpIs36* controls, and sorted into five categories. Large germlines were similar in size and architecture to *cpIs36*, tumorous germlines typically displayed more intense fluorescence but could be difficult to distinguish from large germlines at this resolution, shorts were shorter than control germlines, atrophy was scored as a small pocket of fluorescence near the distal tip of the gonad, and empty was missing Neon Green expression. L4 larvae were selected from sibling sterile plates, singled, and each germline arm was blindly scored daily for germline size on a Leica M205 FA fluorescence microscope.

RNAi Rescue

Late-generation L4 mutants were individually cloned and confirmed to be sterile through day 5. Sterile day 5 worms were then selected and singled to NGM plates with 50 mg/mL ampicillin, 12.5 mg/mL tetracycline, and 1 mM IPTG (RNAi plate condition). These plates were seeded with *E. coli* HT115 expressing dsRNA targeting gene of interest, or an empty vector (L4440), or *E. coli* OP50 (Kamath et al., 2001). The worms were then scored daily for progeny at 20°C. For individual drug reversal experiments, the same drug concentrations found in RNAi plates were added to NGM plates, which were then seeded with OP50 *E. coli*.

RNA Injection/Soaking

RNA was isolated from *E. coli* OP50 seeded on either standard NGM plate or RNAi plate condition using TRIzol Max Bacterial RNA Isolation Kit (Ambion by Life Technologies). RNA presence and quality were confirmed using gel electrophoresis and a Nano Drop spectrophotometer. Total RNA was either injected or soaked into sterile day 5 worms according to published protocols (Fire et al., 1998; Maeda et al., 2001).

Statistical Analysis

Statistical analysis was performed using the R statistical environment (R Core Team, 2017). For *prg-1* sterile-mutant statistical analysis, due to the limitations of obtaining large experimental pools of sterile *prg-1* mutants, worms with low brood sizes were expanded and sterile progeny were collected. Each worm was treated as an individual sterility event, and all data from various pools were aggregated and analyzed. For analysis of germline phenotypes, contingency tables were constructed from the observed frequencies of the different phenotypes. Pairwise chi-square tests or Fisher's exact test were performed to test for significant differences in the distribution of germline phenotypes between different strains/conditions. Bonferroni correction was used to control the familywise error rate when multiple comparisons were made.

SUPPLEMENTAL INFORMATION

Supplemental Information includes Supplemental Experimental Procedures, two figures, and one table and can be found with this article online at https://doi.org/10.1016/j.celrep.2018.03.015.

ACKNOWLEDGMENTS

We thank J. Mitchell for insight into germline remodeling, D. Reiner for suggestions on experimental design and strains, L. Leopold for assistance with

statistical analysis, P. Hu for *daf-2* and *age-1* RNAi clones, M. Jarstfer and members of the Ahmed lab for critical reading of the manuscript, J. Powell-Coffman for lucid comments on ARD exit, and D. Dickinson for the strain *cpls36*. Some strains used in this work were provided by the *Caenorhabditis* Genetics Center, which is funded by the NIH Office of Research Infrastructure Programs (P40 OD010440). B.H., M.S., S.F., D.T., and S.A. were supported by NIH Grant GM083048 to S.A.

AUTHOR CONTRIBUTIONS

B.H., M.S., D.T., and S.A. designed and performed experiments. S.A. supervised the research. B.H., M.S., S.F., and S.A. analyzed data and wrote the paper.

DECLARATION OF INTERESTS

The authors declare no competing interests.

Received: August 9, 2017
Revised: January 24, 2018
Accepted: March 5, 2018
Published: April 3, 2018

REFERENCES

Ahmed, S., and Hodgkin, J. (2000). MRT-2 checkpoint protein is required for germline immortality and telomere replication in *C. elegans*. Nature *403*, 159–164.

Angelo, G., and Van Gilst, M.R. (2009). Starvation protects germline stem cells and extends reproductive longevity in *C. elegans*. Science *326*, 954–958.

Armanios, M., and Blackburn, E.H. (2012). The telomere syndromes. Nat. Rev. Genet. *13*, 693–704.

Bagijn, M.P., Goldstein, L.D., Sapetschnig, A., Weick, E.M., Bouasker, S., Lehrbach, N.J., Simard, M.J., and Miska, E.A. (2012). Function, targets, and evolution of *Caenorhabditis elegans* piRNAs. Science *337*, 574–578.

Batista, P.J., Ruby, J.G., Claycomb, J.M., Chiang, R., Fahlgren, N., Kasschau, K.D., Chaves, D.A., Gu, W., Vasale, J.J., Duan, S., et al. (2008). PRG-1 and 21U-RNAs interact to form the piRNA complex required for fertility in *C. elegans*. Mol. Cell *31*, 67–78.

Baumann, K. (2012). Cell death: multitasking p53 promotes necrosis. Nat. Rev. Mol. Cell Biol. *13*, 480–481.

Blackstone, E., Morrison, M., and Roth, M.B. (2005). H2S induces a suspended animation-like state in mice. Science *308*, 518.

Chen, L., McCloskey, T., Joshi, P.M., and Rothman, J.H. (2008). ced-4 and proto-oncogene tfg-1 antagonistically regulate cell size and apoptosis in *C. elegans*. Curr. Biol. *18*, 1025–1033.

Choi, Y., and Mango, S.E. (2014). Hunting for Darwin's gemmules and Lamarck's fluid: transgenerational signaling and histone methylation. Biochim. Biophys. Acta *1839*, 1440–1453.

Das, P.P., Bagijn, M.P., Goldstein, L.D., Woolford, J.R., Lehrbach, N.J., Sapetschnig, A., Buhecha, H.R., Gilchrist, M.J., Howe, K.L., Stark, R., et al. (2008). Piwi and piRNAs act upstream of an endogenous siRNA pathway to suppress Tc3 transposon mobility in the *Caenorhabditis elegans* germline. Mol. Cell *31*, 79–90.

de Albuquerque, B.F., Placentino, M., and Ketting, R.F. (2015). Maternal piRNAs are essential for germline development following de novo establishment of endo-siRNAs in *Caenorhabditis elegans*. Dev. Cell *34*, 448–456.

De Cecco, M., Criscione, S.W., Peckham, E.J., Hillenmeyer, S., Hamm, E.A., Manivannan, J., Peterson, A.L., Kreiling, J.A., Neretti, N., and Sedivy, J.M. (2013). Genomes of replicatively senescent cells undergo global epigenetic changes leading to gene silencing and activation of transposable elements. Aging Cell *12*, 247–256.

Dernburg, A.F., McDonald, K., Moulder, G., Barstead, R., Dresser, M., and Villeneuve, A.M. (1998). Meiotic recombination in *C. elegans* initiates by a conserved mechanism and is dispensable for homologous chromosome synapsis. Cell *94*, 387–398.

Fire, A., Xu, S., Montgomery, M.K., Kostas, S.A., Driver, S.E., and Mello, C.C. (1998). Potent and specific genetic interference by double-stranded RNA in *Caenorhabditis elegans*. Nature *391*, 806–811.

Gartner, A., Boag, P.R., and Blackwell, T.K. (2008). Germline survival and apoptosis. In WormBook: The Online Review of C. *elegans* Biology (WormBook). https://www.ncbi.nlm.nih.gov/books/NBK116071/.

Golden, J.W., and Riddle, D.L. (1982). A pheromone influences larval development in the nematode *Caenorhabditis elegans*. Science *218*, 578–580.

Golden, J.W., and Riddle, D.L. (1984). The *Caenorhabditis elegans* dauer larva: developmental effects of pheromone, food, and temperature. Dev. Biol. *102*, 368–378.

Gorbunova, V., Boeke, J.D., Helfand, S.L., and Sedivy, J.M. (2014). Human Genomics. Sleeping dogs of the genome. Science *346*, 1187–1188.

He, S., and Sharpless, N.E. (2017). Senescence in health and disease. Cell *169*, 1000–1011.

Hsu, A.L., Murphy, C.T., and Kenyon, C. (2003). Regulation of aging and age-related disease by DAF-16 and heat-shock factor. Science *300*, 1142–1145.

Hughes, S.E., Evason, K., Xiong, C., and Kornfeld, K. (2007). Genetic and pharmacological factors that influence reproductive aging in nematodes. PLoS Genet. *3*, e25.

Juliano, C., Wang, J., and Lin, H. (2011). Uniting germline and stem cells: the function of Piwi proteins and the piRNA pathway in diverse organisms. Annu. Rev. Genet. *45*, 447–469.

Kamath, R.S., Martinez-Campos, M., Zipperlen, P., Fraser, A.G., and Ahringer, J. (2001). Effectiveness of specific RNA-mediated interference through ingested double-stranded RNA in Caenorhabditis elegans. Genome Biol *2*, RESEARCH0002.

Kenyon, C.J. (2010). The genetics of ageing. Nature *464*, 504–512.

Korta, D.Z., Tuck, S., and Hubbard, E.J. (2012). S6K links cell fate, cell cycle and nutrient response in *C. elegans* germline stem/progenitor cells. Development *139*, 859–870.

Maeda, I., Kohara, Y., Yamamoto, M., and Sugimoto, A. (2001). Large-scale analysis of gene function in *Caenorhabditis elegans* by high-throughput RNAi. Curr. Biol. *11*, 171–176.

Malik, H.S., and Henikoff, S. (2002). Conflict begets complexity: the evolution of centromeres. Curr. Opin. Genet. Dev. *12*, 711–718.

McMurchy, A.N., Stempor, P., Gaarenstroom, T., Wysolmerski, B., Dong, Y., Aussianikava, D., Appert, A., Huang, N., Kolasinska-Zwierz, P., Sapetschnig, A., et al. (2017). A team of heterochromatin factors collaborates with small RNA pathways to combat repetitive elements and germline stress. eLife *6*, e21666.

Meier, B., Clejan, I., Liu, Y., Lowden, M., Gartner, A., Hodgkin, J., and Ahmed, S. (2006). trt-1 is the *Caenorhabditis elegans* catalytic subunit of telomerase. PLoS Genet. *2*, e18.

Metzstein, M.M., Stanfield, G.M., and Horvitz, H.R. (1998). Genetics of programmed cell death in *C. elegans*: past, present and future. Trends Genet. *14*, 410–416.

Miller, D.L., and Roth, M.B. (2009). *C. elegans* are protected from lethal hypoxia by an embryonic diapause. Curr. Biol. *19*, 1233–1237.

Nystul, T.G., Goldmark, J.P., Padilla, P.A., and Roth, M.B. (2003). Suspended animation in *C. elegans* requires the spindle checkpoint. Science *302*, 1038–1041.

Ogg, S., and Ruvkun, G. (1998). The *C. elegans* PTEN homolog, DAF-18, acts in the insulin receptor-like metabolic signaling pathway. Mol. Cell *2*, 887–893.

Padilla, P.A., and Ladage, M.L. (2012). Suspended animation, diapause and quiescence: arresting the cell cycle in *C. elegans*. Cell Cycle *11*, 1672–1679.

Phillips, C.M., Brown, K.C., Montgomery, B.E., Ruvkun, G., and Montgomery, T.A. (2015). piRNAs and piRNA-dependent siRNAs protect conserved and essential *C. elegans* genes from misrouting into the RNAi pathway. Dev. Cell *34*, 457–465.

Pinkston-Gosse, J., and Kenyon, C. (2007). DAF-16/FOXO targets genes that regulate tumor growth in *Caenorhabditis elegans*. Nat. Genet. *39*, 1403–1409.

R Core Team (2017). R: A Language and Environment for Statistical Computing (R Foundation for Statistical Computing). https://www.R-project.org/.

Ragland, G.J., Denlinger, D.L., and Hahn, D.A. (2010). Mechanisms of suspended animation are revealed by transcript profiling of diapause in the flesh fly. Proc. Natl. Acad. Sci. USA *107*, 14909–14914.

Ratnappan, R., Amrit, F.R., Chen, S.W., Gill, H., Holden, K., Ward, J., Yamamoto, K.R., Olsen, C.P., and Ghazi, A. (2014). Germline signals deploy NHR-49 to modulate fatty-acid β-oxidation and desaturation in somatic tissues of *C. elegans*. PLoS Genet. *10*, e1004829.

Roy, D., Michaelson, D., Hochman, T., Santella, A., Bao, Z., Goldberg, J.D., and Hubbard, E.J. (2016). Cell cycle features of *C. elegans* germline stem/progenitor cells vary temporally and spatially. Dev. Biol. *409*, 261–271.

Sakaguchi, A., Sarkies, P., Simon, M., Doebley, A.L., Goldstein, L.D., Hedges, A., Ikegami, K., Alvares, S.M., Yang, L., LaRocque, J.R., et al. (2014). *Caenorhabditis elegans* RSD-2 and RSD-6 promote germ cell immortality by maintaining small interfering RNA populations. Proc. Natl. Acad. Sci. USA *111*, E4323–E4331.

Schiesari, L., and O'Connor, M.B. (2013). Diapause: delaying the developmental clock in response to a changing environment. Curr. Top. Dev. Biol. *105*, 213–246.

Schumacher, B., Hofmann, K., Boulton, S., and Gartner, A. (2001). The *C. elegans* homolog of the p53 tumor suppressor is required for DNA damage-induced apoptosis. Curr. Biol. *11*, 1722–1727.

Seidel, H.S., and Kimble, J. (2011). The oogenic germline starvation response in *C. elegans*. PLoS One *6*, e28074.

Seidel, H.S., and Kimble, J. (2015). Cell-cycle quiescence maintains *Caenorhabditis elegans* germline stem cells independent of GLP-1/Notch. eLife *4*, e10832.

Sharpless, N.E., and DePinho, R.A. (2007). How stem cells age and why this makes us grow old. Nat. Rev. Mol. Cell Biol. *8*, 703–713.

Simon, M., Sarkies, P., Ikegami, K., Doebley, A.L., Goldstein, L.D., Mitchell, J., Sakaguchi, A., Miska, E.A., and Ahmed, S. (2014). Reduced insulin/IGF-1 signaling restores germ cell immortality to *Caenorhabditis elegans* Piwi mutants. Cell Rep. *7*, 762–773.

Smelick, C., and Ahmed, S. (2005). Achieving immortality in the *C. elegans* germline. Ageing Res. Rev. *4*, 67–82.

Spracklin, G., Fields, B., Wan, G., Becker, D., Wallig, A., Shukla, A., and Kennedy, S. (2017). The RNAi inheritance machinery of *Caenorhabditis elegans*. Genetics *206*, 1403–1416.

Strome, S., and Updike, D. (2015). Specifying and protecting germ cell fate. Nat. Rev. Mol. Cell Biol. *16*, 406–416.

Syntichaki, P., Xu, K., Driscoll, M., and Tavernarakis, N. (2002). Specific aspartyl and calpain proteases are required for neurodegeneration in *C. elegans*. Nature *419*, 939–944.

Tatar, M., and Yin, C. (2001). Slow aging during insect reproductive diapause: why butterflies, grasshoppers and flies are like worms. Exp. Gerontol. *36*, 723–738.

Van Gilst, M.R., Hadjivassiliou, H., Jolly, A., and Yamamoto, K.R. (2005a). Nuclear hormone receptor NHR-49 controls fat consumption and fatty acid composition in *C. elegans*. PLoS Biol. *3*, e53.

Van Gilst, M.R., Hadjivassiliou, H., and Yamamoto, K.R. (2005b). A *Caenorhabditis elegans* nutrient response system partially dependent on nuclear receptor NHR-49. Proc. Natl. Acad. Sci. USA *102*, 13496–13501.

Van Meter, M., Kashyap, M., Rezazadeh, S., Geneva, A.J., Morello, T.D., Seluanov, A., and Gorbunova, V. (2014). SIRT6 represses LINE1 retrotransposons by ribosylating KAP1 but this repression fails with stress and age. Nat. Commun. *5*, 5011.

Vowels, J.J., and Thomas, J.H. (1992). Genetic analysis of chemosensory control of dauer formation in *Caenorhabditis elegans*. Genetics *130*, 105–123.

Zeller, P., Padeken, J., van Schendel, R., Kalck, V., Tijsterman, M., and Gasser, S.M. (2016). Histone H3K9 methylation is dispensable for *Caenorhabditis elegans* development but suppresses RNA:DNA hybrid-associated repeat instability. Nat. Genet. *48*, 1385–1395.

Zhou, Z., Hartwieg, E., and Horvitz, H.R. (2001). CED-1 is a transmembrane receptor that mediates cell corpse engulfment in *C. elegans*. Cell *104*, 43–56.

Zhou, K.I., Pincus, Z., and Slack, F.J. (2011). Longevity and stress in *Caenorhabditis elegans*. Aging (Albany N.Y.) *3*, 733–753.

Cell Reports, Volume *23*

Supplemental Information

Transgenerational Sterility of Piwi Mutants Represents a Dynamic Form of Adult Reproductive Diapause

Bree Heestand, Matt Simon, Stephen Frenk, Denis Titov, and Shawn Ahmed

SUPPLEMENTAL EXPERIMENTAL PROCEDURES

Strains used include Bristol N2 wild type, *dpy-5(e61) I*, *unc-13(e450) I*, *prg-1(n4357) I, prg-1(tm876) I, cpIs36[Pmex-5::mNeonGreen::3xFlag::AraD::tbb-2 3'UTR + unc-119(+)] II; unc-119(ed3) III, unc-29(e193) I*, *daf-16(mg50) I, daf-16(mu86) I*, *hsf-1 (sy441) I*, *nhr-49 (nr2041) I, nhr-49 (ok2165)* I, *cep-1 (w40), cep-1 (gk130) I*, *daf-2 (e1368) III, daf-2(e1370) III, daf-2(m41) III*, *ced-4(n1162) III*, *dpy-17(e164) III*, *daf-18(e1375), daf-18(ok480) IV, dpy-9(e12) IV*, *unc-24(e120) IV*, *ced-3(n717) IV, crt-1 (jh101), mut-7 (pk204) III, Pced-1::ced-1::gfp*.

Note that we previously found that sterile generation *prg-1* mutant adults that were sterile on the second day of adulthood remained sterile when grown on standard NGM plates seeded with OP50 bacteria. Fertility could be restored for a fraction of these animals that were placed specifically on RNAi plates expressing dsRNA targeting *daf-2* or the downstream PI3 kinase subunit *age-1,* but fertility did not occur on vector control RNAi plates (Simon et al., 2014). These results contrast with our current results that show that complete sterility does not occur for sterile-generation *prg-1* adults until Day 5 of adulthood, and that fertility can be restored to a small fraction of Day 5 sterile adults that are placed on RNAi plates containing any type of RNAi bacteria. We do not have an explanation for these differences, but note that our present results have been independently repeated using numerous *prg-1* mutants lines and high n values per experiment, suggesting that the observed differences could be due to changes in the metabolic environment in the lab (Schulenburg and Felix, 2017).

SUPPLEMENTAL REFERENCES

Schulenburg, H., and Felix, M.A. (2017). The Natural Biotic Environment of Caenorhabditis elegans. Genetics *206*, 55-86.

Supplemental Figure 1

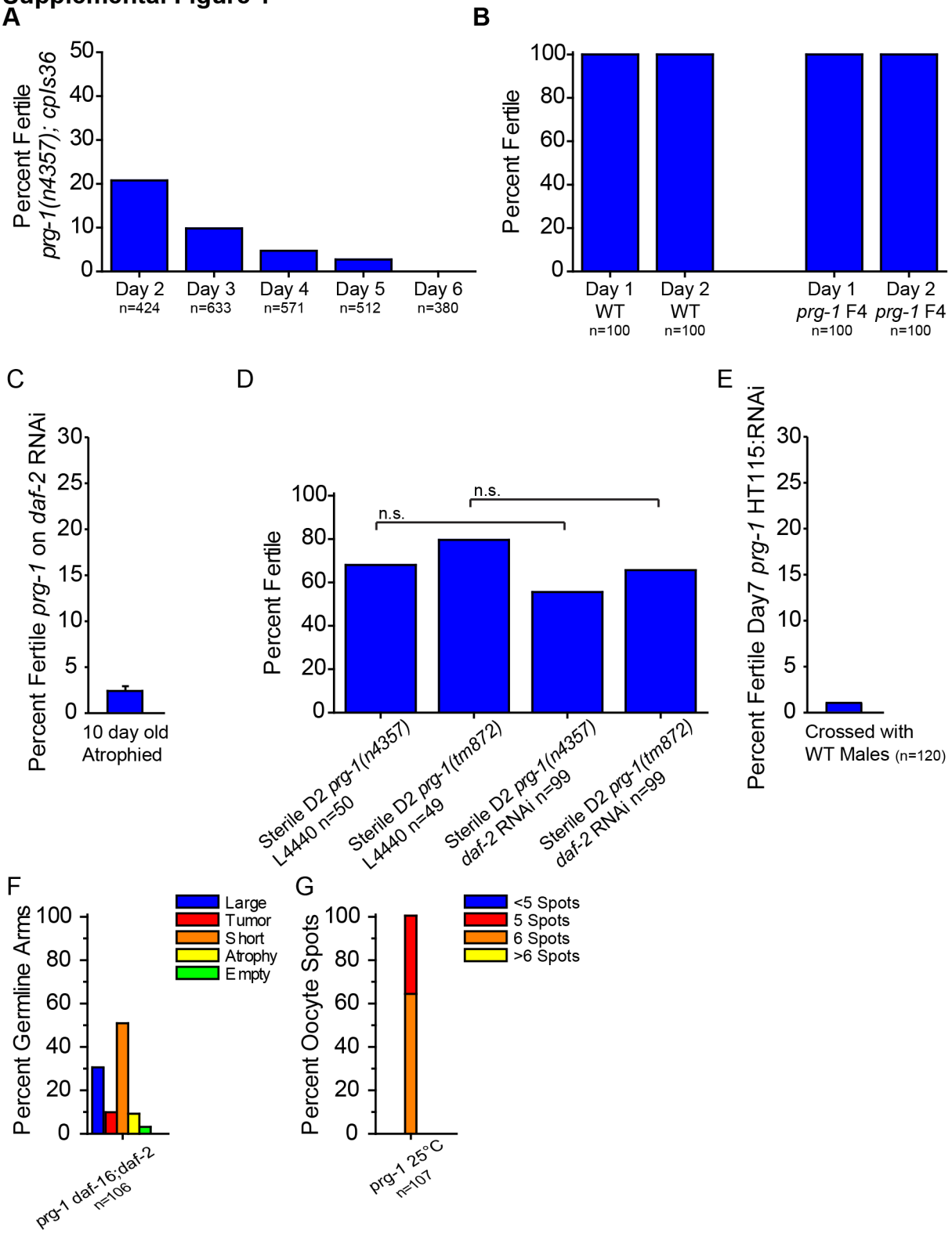

Supplemental Figure S1. Related to Figures 1 and 5. Fertility of *prg-1* mutants. (A) Sterile Day one *prg-1; cpIs36* mutants reverse sterility through the first five days of adulthood. (B) Early generation *prg-1* mutants (F4) are completely fertile. (C) *prg-1* mutants who had been sterile for ten days become fertile on RNAi bacteria targeting

daf-2. Error bars are S.E.M. (D) Percent fertile of 2 alleles of Day 2 sterile *prg-1*. n=total worms scored. *daf-2* RNAi had no significant effect on percent fertile (p=n.s., Chi-square test with Bonferroni correction). (E) Crossing with wild-type males did not enhance reversal of sterility of sterile Day 7 *prg-1* mutants in the HT115 RNAi condition. (F) Germline profile of *prg-1 daf-16; daf-2* Day 1 sterile mutants. (G) Number of DAPI spots in sterile Day 1 *prg-1* mutant worms at 25°C.

Supplemental Figure 2

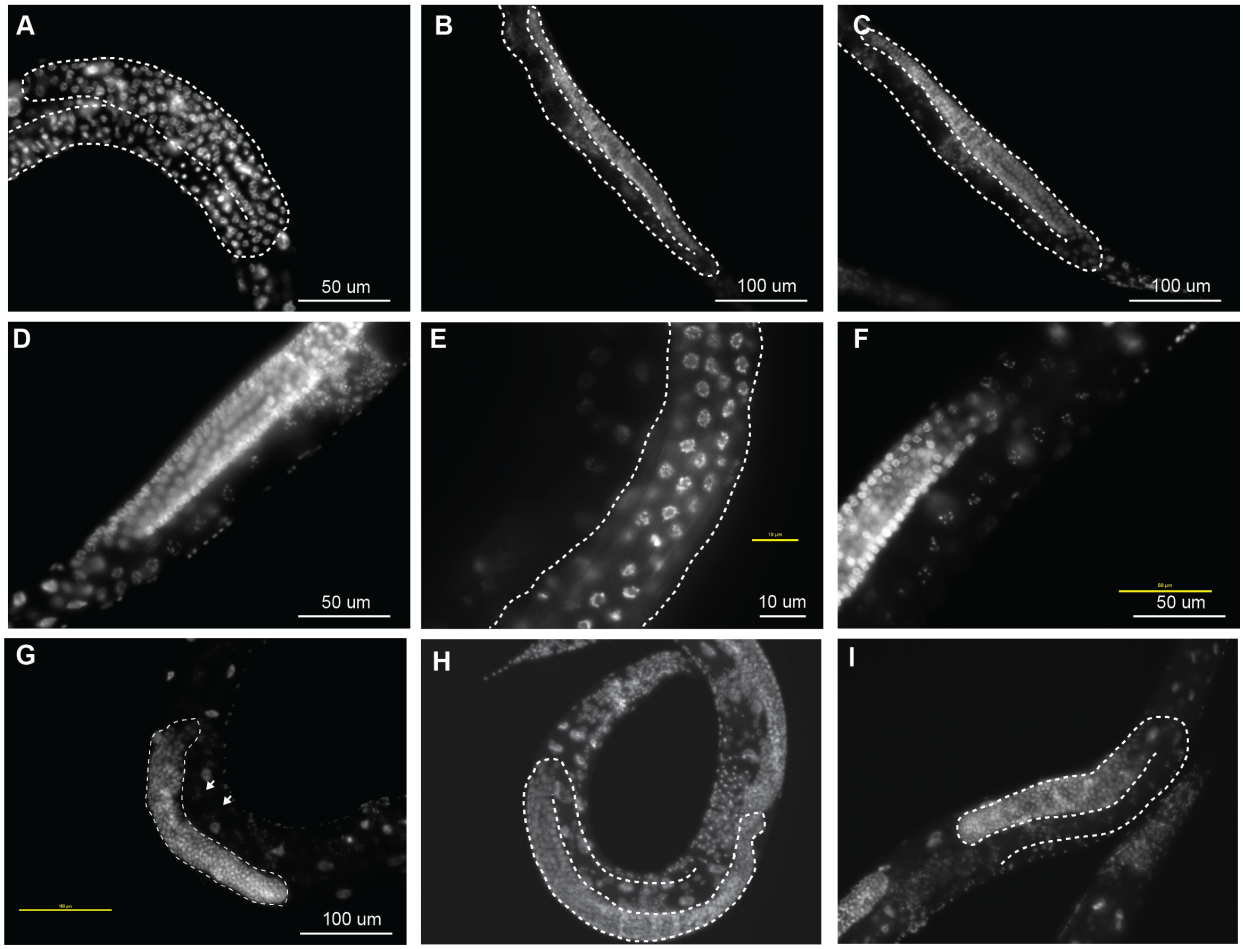

Supplemental Figure S2. Related to Figure 2. Germline atrophy in sterile *prg-1* animals. DAPI-stained photos of (A) a *prg-1* early generation L4, (B) *prg-1* early generation fertile adult, (C) a N2 wild-type adult, (D) a *prg-1* early generation adult with mitotic-meiotic transition and normal oocyte production, (E) mitotic cells in a likely sterile *prg-1* L4, (F) a rare sterile *prg-1* animal with intact germline lacking embryo production, (G) *a prg-1 daf-16* sterile adult with oocytes indicated by arrows, (H) N2 wild-type germline showing full bend, (I) sterile *prg-1* large germline showing early bend.

p values determined using Chi-squared with Bonferroni correction

	N2 (n=87)	prg-1 (n=483)	prg-1; ced-3 (n=310)	prg-1; ced-4 (n=552)	prg-1, cep-1 (n=229)	prg-1; nhr-49 (n=194)	prg-1 haf-1 (n=169)	prg-1 daf-16 (n=169)	prg-1; daf-18 (n=377)	prg-1 daf-16; ced-4 (n=252)	prg-1 nhr-49; ced-4 (n=195)	prg-1 cep-1; daf-18 (n=180)
N2 (n=87)		1.04743E-73	3.21872E-26	8.62893E-30	1.18329E-13	4.24406E-36	9.34428E-32	9.08427E-32	4.37486E-51	2.39832E-52	6.07126E-30	1.28658E-08
***prg-1* (n=483)**	1.04743E-73		9.75882E-20	1.91748E-47	1.09518E-44	2.23708E-28	2.60034E-37	3.25497E-49	3.00924E-41	7.0185E-40	2.29352E-18	7.41608E-53
***prg-1; ced-3* (n=310)**	3.21872E-26	9.75882E-20		0.032842055	6.91215E-05	6.26089E-07	3.18166E-12	5.43015E-18	8.74289E-13	6.88607E-18	0.137269472	6.61644E-10
***prg-1; ced-4* (n=552)**	8.62893E-30	1.91748E-47	0.032842055		6.30262E-05	6.26089E-07	1.31003E-07	9.47228E-13	2.05963E-11	1.11006E-16	0.089538857	1.53227E-07
***prg-1 cep-1* (n=229)**	1.18329E-13	1.09518E-44	6.91215E-05	6.30262E-05		7.37602E-15	9.55472E-13	5.92393E-18	1.0168E-22	1.9949E-27	8.7906E-07	0.12579811
***prg-1 nhr-49* (n=194)**	4.24406E-36	2.23708E-28	6.26089E-07	0.000260344	7.37602E-15		0.0285444	0.005614851	1	0.472692318	0.571308717	3.18579E-14
***prg-1 haf-1* (n=169)**	9.34428E-32	2.60034E-37	3.18166E-12	1.31003E-07	9.55472E-13	0.0285444		1	1	0.022315436	0.060957594	1.20143E-12
***prg-1 daf-16* (n=169)**	9.08427E-32	3.25497E-49	5.43015E-18	9.47228E-13	5.92393E-18	0.005614851	1		0.183721705	0.021752563	4.33676E-05	4.36191E-13
***prg-1; daf-18* (n=377)**	4.37486E-51	3.00924E-41	8.74289E-13	2.05963E-11	1.0168E-22	1	1	0.183721705		1	0.46985913	5.16183E-23
***prg-1 daf-16; ced-4* (n=252)**	2.39832E-52	7.0185E-40	6.88607E-18	1.11006E-16	1.9949E-27	0.472692318	0.022315436	0.021752563	1		0.00020915	1.2455E-26
***prg-1 nhr-49; ced-4* (n=195)**	6.07126E-30	2.29352E-18	0.137269472	0.089538857	8.7906E-07	0.571308717	0.060957594	4.33676E-05	0.46985913	0.00020915		6.45661E-11
***prg-1 cep-1; daf-18* (n=180)**	1.28658E-08	7.41608E-53	6.61644E-10	1.53227E-07	0.12579811	3.18579E-14	1.20143E-12	4.36191E-13	5.16183E-23	1.2455E-26	6.45661E-11	

	N2	prg-1	prg-1 cep-1	prg-1; crt-1	prg-1 cep-1; crt-1	prg-1 cep-1; ced-3	prg-1 cep-1; ced-4
N2		3.33272E-74	3.765E-14	3.99493E-12	7.37112E-39	0.000770494	2.97502E-39
prg-1	3.33272E-74		3.48466E-45	3.01222E-46	9.06566E-72	9.88018E-76	3.82783E-40
prg-1 cep-1	3.765E-14	3.48466E-45		0.002462576	4.00033E-21	1.28993E-07	1.53162E-19
prg-1; crt-1	3.99493E-12	3.01222E-46	0.002462576		2.76165E-07	0.000126617	1.69351E-16
prg-1 cep-1; crt-1	7.37112E-39	9.06566E-72	4.00033E-21	2.76165E-07		7.58376E-35	4.42727E-18
prg-1 cep-1; ced-3	0.000770494	9.88018E-76	1.28993E-07	0.000126617	7.58376E-35		2.7317E-34
prg-1 cep-1; ced-4	2.97502E-39	3.82783E-40	1.53162E-19	1.69351E-16	4.42727E-18	2.7317E-34	

Supplemental Table S1. Related to Figures 1 and 5. Significance values for germline profile comparisons. Related to Figure 1D and 5C. P values for germline arm profiles were determined using pairwise Chi-square tests with Boferroni correction.